

Co-Design to Enable User-Friendly Tools to Assess the Impact of Future Mobility Solutions

Gioele Zardini¹, Nicolas Lanzetti², Andrea Censi¹, Emilio Frazzoli¹, and Marco Pavone³

Abstract—The design of future mobility solutions and the design of the mobility systems they enable are closely coupled. Indeed, knowledge about the intended service of novel mobility solutions would impact their design and deployment process, whilst insights about their technological development could significantly affect transportation management policies. This requires tools to study such a coupling and co-design mobility systems in terms of different objectives. We present a framework to address such co-design problems, leveraging a mathematical theory of co-design to frame and solve the problem of designing and deploying an intermodal mobility system, whereby autonomous vehicles service travel demands jointly with micromobility solutions and public transit, in terms of fleets sizing, vehicle characteristics, and public transit service frequency. Our framework is modular and compositional, allowing one to describe the design as the interconnection of simple components and to tackle it from a systemic perspective. Moreover, it requires general monotonicity assumptions and naturally handles multiple objectives, delivering rational, actionable solutions for policy makers. We showcase our methodology in a case study of Washington D.C., USA. Our work suggests the possibility to create user-friendly optimization tools to systematically assess costs and benefits of interventions, and to inform policy-making in the future.

Index Terms—Network optimization and control, Network resource allocation, Complex Networks, Cyber-Physical Network Co-Design and Analysis, Transportation Systems Analysis, Service network design, planning, and scheduling, Transportation infrastructure and investment, Emerging topics in transportation and logistics networks

I. INTRODUCTION

Current transportation systems are undergoing dramatic mutations, arising from the deployment of novel mobility solutions, such as autonomous vehicles (AVs) and micromobility (μ M) systems. New mobility paradigms promise to drastically reduce negative externalities produced by the transportation system, such as emissions, travel time, parking spaces and, critically, fatalities (for a review on the subject, refer to [1]). However, industrial experience shows that the current design process for new mobility solutions often suffers from the lack of clear, specific requirements in terms of the service they will be providing [2]. Yet, knowledge about their intended service (e.g., last-mile versus point-to-point travel) might dramatically

impact how vehicles are designed and significantly ease their development process. For instance, if for a given city we knew that for an effective on-demand mobility system AVs only need to drive up to 30 mph and only on relatively simple roads, their design would be greatly simplified and their deployment could be accelerated. Furthermore, from the system-level perspective of transportation management, knowledge about the trajectory of technology development for new mobility solutions would certainly impact decisions on future infrastructure investments and provisions of service. In other words, the design of future mobility solutions and the design of a mobility system leveraging them are intimately *coupled*. This calls for methods to reason about such a coupling, and in particular to *co-design* the individual mobility solutions and the associated mobility systems. A key requirement in this context is to be able to account for a range of heterogeneous objectives that are often not directly comparable (consider, for instance, travel time, public expense, and externalities), to formulate hierarchical design problems involving different disciplines, and to solve them in a computationally tractable manner.

Accordingly, the goal of this paper is to lay the foundations for a framework through which one can systematically co-design future mobility systems. Specifically, we show how to leverage a recently developed monotone theory of co-design [3]–[6], which provides a general methodology to co-design complex systems in a modular and compositional fashion [7], [8]. This tool delivers the set of rational design solutions lying on the Pareto front, allowing one to reason about costs and benefits of the individual design options. The framework is instantiated in the setting of co-designing intermodal mobility systems [9], whereby fleets of self-driving vehicles provide on-demand mobility jointly with fleets of micromobility vehicles (μ MVs) such as e-scooters (ESs), shared bikes (SBs), mopeds (Ms) and fuel-cell mopeds (FCMs), and public transit. Aspects that are subject to co-design include fleet sizes, vehicle-specific characteristics for AVs and μ MVs, and service features, such as public transit service frequency, prices, and serviced networks.

A. Related Literature

Our work lies at the interface of the design of public transportation services and the design of novel mobility solutions.

The first research stream is reviewed in [10]–[12] and comprises *strategic* long-term infrastructure modifications and *operational* short-term scheduling. The joint design of traffic network topology and control infrastructure has been presented in [13], [14]. Public transportation scheduling has been solved jointly with the design of the transit network by optimizing

¹Institute for Dynamic Systems and Control, ETH Zürich, Zürich (ZH), Switzerland {gzardini, acensi, emilio.frazzoli}@ethz.ch

²Automatic Control Laboratory, ETH Zürich, Zürich (ZH), Switzerland, nicolas@ethz.ch

³Department of Aeronautics and Astronautics, Stanford University, Stanford (CA), United States, pavone@stanford.edu

This work was supported by the National Science Foundation under CAREER Award CMMI-1454737, and by the Swiss National Science Foundation under NCCR Automation, grant agreement 51NF40_180545. This article solely reflects the opinions and conclusions of its authors and not NSF, NCCR, or any other entity.

passengers' and operators' costs in [15], the satisfied demand in [16], and the energy consumptions of the system in [17]. However, these works mainly focus on a single infrastructure (road network or public transportation), and do not consider its joint design with new mobility solutions.

The research on novel mobility solutions mainly pertains to AVs, Autonomous Mobility-on-Demand (AMoD) systems, and μ M. The research on design of AMoD systems is thoroughly reviewed in [1] and references therein, and mainly concerns their fleet sizing. In this regard, existing studies range from simulation-based approaches [18]–[23] to analytical methods [24]. In [25], the fleet size and the charging infrastructure of an AMoD system are jointly designed, and the arising design problem is formulated as a mixed integer linear program. In [26], the fleet sizing problem is solved together with the vehicle allocation problem. Furthermore, [27] proposes a framework to jointly design the AMoD fleet size and its composition. More recently, the joint design of multi-modal transit networks and AMoD systems was formulated in [28] as a bilevel optimization problem and solved with heuristics, and coupled with infrastructure design in [29], using multi-objective linear optimization. Overall, the problem-specific structure of existing design methods for AMoD systems is often not amenable to a modular and compositional problem formulation. Furthermore, key AV characteristics, such as the achievable speed, are not considered. Research on the design and impact of μ M solutions has been reviewed in [30], which focuses on the urban deployment of SBs and ESs. In particular, [31] presents a design framework for a multi-modal public transportation system, including various μ M solutions and buses, optimizing user preferences and social costs. Fleet deployment models are analyzed in [32]–[35]. The optimal allocation of SBs in a city is studied through mathematical programming models in [32], and solved through stochastic optimization in [33], [34]. Finally, [36] explores the impact of μ M on urban planning and identifies strategies to increase μ MVs utilization.

At a higher abstraction level, the problem we are trying to solve matches some of the principles of collaborative engineering [37], [38], which, while providing interesting insights, do not offer a mathematical theory and a scalable computational framework to deal with hierarchical, multi-objective design problems.

In conclusion, to the best of the authors' knowledge, the existing design frameworks for mobility systems have a fixed problem-specific structure, and therefore do not permit to *co-design* the mobility infrastructure in a modular and compositional manner. Moreover, previous works neither capture important aspects of future mobility systems, such as the interactions among different transportation modes, nor specific design parameters of novel mobility solutions, as for instance the level of autonomy and the serviced network of AVs, in a computationally tractable and compositional way.

B. Statement of contributions

In this paper, we lay the foundations for the systematic study of the design of future mobility systems. Specifically, we leverage a mathematical theory of co-design [3], [6] to

devise a framework to study the design of intermodal mobility systems in terms of mobility solutions and fleet characteristics, enabling the computation of the *rational* solutions lying on the Pareto front of minimal travel time, transportation costs, and externalities. Our framework paves the way to structure the design problem in a modular way, in which each different transportation option can be “plugged in” in a larger model. Each model has minimal assumptions: Rather than properties such as linearity, continuity, or convexity, we ask for very general monotonicity assumptions, proven to be reasonable in the present paper and in previous works [5], [7], [8]. For example, we assume that the cost of automation of an AV does not decrease with the increase of the speed achievable by the AV. We are able to obtain the full Pareto front of *rational* solutions or, given policies, to weigh incomparable costs (such as travel time and emissions) and to present actionable information to the stakeholders of the mobility ecosystem. We consider the case study of Washington D.C., USA, to showcase our methodology. We illustrate how, given the model, we can easily formulate and answer several questions regarding the introduction of new technologies and investigate possible infrastructure interventions. This article significantly extends the preliminary material previously presented in [39], [40]. In particular, we first broaden and extend the formal presentation of the mathematical theory of co-design, and detail its application in this work by formalizing the introduced design problems (including proofs, new insights, and generalizability of the approach). Second, we extend the discussion of the literature, including recent research pertaining to the co-design of future mobility systems, with a focus on μ M. Third, we showcase the modularity of our framework by including the design of μ M solutions (both at the vehicle and at the fleet level) in the future mobility co-design problem, and evaluate their impact on the transportation system for the case study of Washington D.C., USA, whereby we leverage the network of the city, as well as demand datasets. Furthermore, we include a study of pricing strategies in the mobility co-design problem, highlighting the flexibility of the proposed framework. Finally, we extend our case studies with further scenarios and provide new managerial insights.

C. Organization of the paper

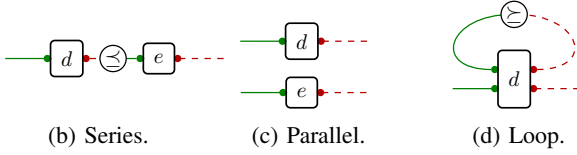
The remainder of this paper is structured as follows: Section II reviews the mathematical background on which our framework is based. Section III presents models for future mobility systems and related co-design problems, by introducing the single design problems (DPs) and their interconnection forming a co-design problem (CDP). We showcase our methodology with several case studies for Washington D.C., USA, in Section IV. Section V concludes the paper with a discussion and an overview on future research directions. Nomenclature is available in the appendix.

II. MONOTONE CO-DESIGN THEORY

In this section, we present the main concepts related to the mathematical theory of co-design, presented in [3], [4] and extensively in [6]. We will recall basic concepts of order



(a) A monotone design problem with implementation (MDPI) is a monotone relation between partially ordered sets (posets) of **functionalities** and **resources**.



(b) Series. (c) Parallel. (d) Loop.

Fig. 1: MDPIs can be composed in different ways.

theory along the way. For more details, the interested reader is referred to [41].

The plot of the section is the following. We will introduce a theory of co-design whose atoms are MDPIs, which are (monotone) feasibility relations between functionalities and resources. We will then explain how one can compose MDPIs in various ways, define optimization problems related to the introduced structures, and hint at the solution techniques (with details reported in the Appendix B for convenience).

Resources in this theory are quantified via partially ordered sets (posets).

Definition II.1 (Poset). A *poset* is a tuple $\mathcal{P} = \langle P, \preceq_{\mathcal{P}} \rangle$, where P is a set and $\preceq_{\mathcal{P}}$ is a partial order, defined as a reflexive, transitive, and antisymmetric relation.

This structure allows one to describe standard engineering quantities (typically totally ordered sets), such as $\langle \mathbb{R}_{\geq 0}, \leq \rangle$ (e.g., energy, costs) and $\langle \mathbb{N}, \leq \rangle$ (e.g., number of vehicles in a fleet), but also more complex ones, which we will introduce later in this work.

Given a poset, we can consider its “reversed” version.

Definition II.2 (Opposite of a poset). The *opposite* of a poset $\mathcal{P} = \langle P, \preceq_{\mathcal{P}} \rangle$ is the poset $\langle P, \preceq_{\mathcal{P}}^{\text{op}} \rangle$, which has the same elements as \mathcal{P} , and the reverse ordering.

To be able to define MDPIs, we further need to introduce the notions of product poset and of monotone map.

Definition II.3 (Product poset). Let $\langle P, \preceq_{\mathcal{P}} \rangle$ and $\langle Q, \preceq_{\mathcal{Q}} \rangle$ be posets. Then, $\mathcal{P} \times \mathcal{Q} = \langle P \times Q, \preceq_{\mathcal{P} \times \mathcal{Q}} \rangle$, with

$$\langle p_1, q_1 \rangle \preceq_{\mathcal{P} \times \mathcal{Q}} \langle p_2, q_2 \rangle \Leftrightarrow p_1 \preceq_{\mathcal{P}} p_2 \text{ and } q_1 \preceq_{\mathcal{Q}} q_2,$$

for all $p_1, p_2 \in \mathcal{P}$, $q_1, q_2 \in \mathcal{Q}$, is the *product poset* of $\langle P, \preceq_{\mathcal{P}} \rangle$ and $\langle Q, \preceq_{\mathcal{Q}} \rangle$.

Definition II.4 (Monotone map). A map $f : \mathcal{P} \rightarrow \mathcal{Q}$ between two posets $\langle P, \preceq_{\mathcal{P}} \rangle$, $\langle Q, \preceq_{\mathcal{Q}} \rangle$ is *monotone* iff $x \preceq_{\mathcal{P}} y$ implies $f(x) \preceq_{\mathcal{Q}} f(y)$. Note that monotonicity is compositional.

We are now ready to define the main atom of the monotone co-design theory.

Definition II.5 (MDPI). Given the posets \mathcal{F}, \mathcal{R} , representing **functionalities** and **resources**, respectively, we define a *monotone design problem with implementation (MDPI)* as a

tuple $\langle \mathcal{I}_d, \text{prov}, \text{reqs} \rangle$, where \mathcal{I}_d is the set of implementations, and prov, reqs are functions from \mathcal{I}_d to \mathcal{F} and \mathcal{R} , respectively:

$$\mathcal{F} \xleftarrow{\text{prov}} \mathcal{I}_d \xrightarrow{\text{reqs}} \mathcal{R}.$$

(Maps prov, reqs are mnemonics for the fact that each implementation *provides* some functionality and *requires* some resources.) We compactly denote the MDPI as $d : \mathcal{F} \rightarrow \mathcal{R}$. Furthermore, to each MDPI we associate a monotone map \bar{d} , given by:

$$\bar{d} : \mathcal{F}^{\text{op}} \times \mathcal{R} \rightarrow \langle \mathcal{P}(\mathcal{I}_d), \subseteq \rangle$$

$$\langle f^*, r \rangle \mapsto \{i \in \mathcal{I}_d : (\text{prov}(i) \succeq_{\mathcal{F}} f) \wedge (\text{reqs}(i) \preceq_{\mathcal{R}} r)\},$$

where $(\cdot)^{\text{op}}$ reverses the order of a poset. We represent a MDPI in diagrammatic form as in Figure 1a.

Remark (Intended semantics for MDPIs). The expression $\bar{d}(f^*, r)$ returns the set of implementations (design choices) $S \subseteq \mathcal{I}_d$ for which the functionalities f are feasible with resources r . For instance, a battery provides **energy**, requires **mass** and has a **cost**. Different battery models represent different implementations.

Remark (Monotonicity of MDPIs). Consider an MDPI with $\bar{d}(f^*, r) = S$.

- Consider $f' \preceq f$. Then, $\bar{d}(f'^*, r) = S' \supseteq S$. In other words, decreasing the desired functionality cannot increase the required resources.
- Consider $r' \succeq r$. Then, $\bar{d}(f^*, r') = S'' \supseteq S$. In other words, increasing the available resources cannot decrease the provided functionalities.

For further related examples, refer to [6].

Individual MDPIs can be composed in several ways to form a co-design problem (Figure 1), allowing one to decompose a large problem into smaller subproblems, and to interconnect them. We report technical details in the appendix, and give a practical intuition in the following. Series composition represents the case in which the functionality of a MDPI is required by another MDPI. For instance, the energy provided by a battery is required by an electric motor to produce torque. The posetal relation “ \preceq ” in Figure 1 represents a co-design constraint: The resource one component requires can be at most as much as the one provided by another component. Parallel composition formalizes decoupled processes happening together. Finally, loop composition describes feedback.¹ The composition operations preserve monotonicity, meaning that the composition of two MDPIs is a MDPI. We call the composition of MDPIs a co-design problem with implementation (CDPI) [3], [5].

We can now formulate problems and describe solutions. Given a poset, we formalize the idea of “Pareto front” via antichains, which are useful to describe incomparable designs.

Definition II.6 (Antichains). A subset $S \subseteq \mathcal{P}$ of a poset \mathcal{P} is an *antichain* iff no elements are comparable: For $x, y \in S$, $x \preceq_{\mathcal{P}} y$ implies $x = y$. We denote by $A\mathcal{P}$ the set of all antichains in \mathcal{P} .

¹It can be proved that the formalization of feedback makes the category of MDPIs a traced monoidal category [6], [42].

Definition II.7 (Functionality to resources map). Given an MDPI d , one can define a monotone map $h_d: \mathcal{F} \rightarrow \mathcal{AR}$, mapping a functionality to the *minimum* antichain of resources providing it. Dually, one can define $h'_d: \mathcal{R} \rightarrow \mathcal{AF}$, mapping a resource to the maximum antichain of functionalities provided by it.

In the design of battery models, h_d maps a particular desired energy to the antichain of masses and costs of (incomparable) battery models providing at least that energy.

We are now ready to state the problem.

Problem 1. We are given a CDPI (interconnection of MDPIs) with functionalities \mathcal{F} and resources \mathcal{R} , and we can evaluate the map h_d for each MDPI d involved. Given a functionality $f \in \mathcal{F}$ of the CDPI, we wish to find the *minimal* resources in \mathcal{R} , for which there exists a feasible implementation vector which makes all sub-problems feasible simultaneously, and all co-design constraints satisfied; or, if none exist, we want to provide a certificate of infeasibility.

In other words, given the maps h_d for the subproblems, we want to evaluate the map h for the entire CDPI.

If h is Scott continuous, and the posets are complete partial orders, one can rely on Kleene's fixed point theorem to find the solution for the interconnected optimization problem [4]. Problem 1 as an instance of a multi-objective optimization problem, which does not require the objectives to be convex, differentiable, continuous, or even defined on continuous spaces. This class of problems can be solved recursively, and their complexity is linear in the number of design options, not combinatorial. These computational properties, and the ease of modeling within the proposed framework, make CDPIs a class of hierarchical multi-objective optimization problems that is computationally scalable, modular, and easily composable. For convenience, we report a detailed description of the solution techniques and their complexity in Appendix B.

Remark (A user-friendly framework). The theory presented in this section and in Appendix B might seem complex. However, it represents the developer-view, as opposed to the optimization framework's user-view. As a user, one just needs to decompose the problem at hand in smaller problems, formulate them as MDPIs (via analytical relations, catalogues, and simulations), and formalize their interconnections. (A user can also focus on a single MDPI and interconnect it with other users' ones). We will show how, once the problem is formulated, a ready-to-use solver will smoothly provide the solutions to custom queries.

III. CO-DESIGN OF FUTURE MOBILITY SYSTEMS

In this section, we detail our co-design framework for future mobility systems, and instantiate it for the specific case of an intermodal transportation network.

A. Intermodal Mobility Framework

1) *Multi-Commodity Flow Model*: The transportation system and its different modes are modeled using the edge-labeled digraph $\mathcal{G} = \langle \mathcal{V}, \mathcal{A}, c \rangle$, sketched in Figure 2. It is described through a set of nodes \mathcal{V} and a set of arcs $\mathcal{A} \subseteq \mathcal{V} \times \mathcal{V}$, labeled

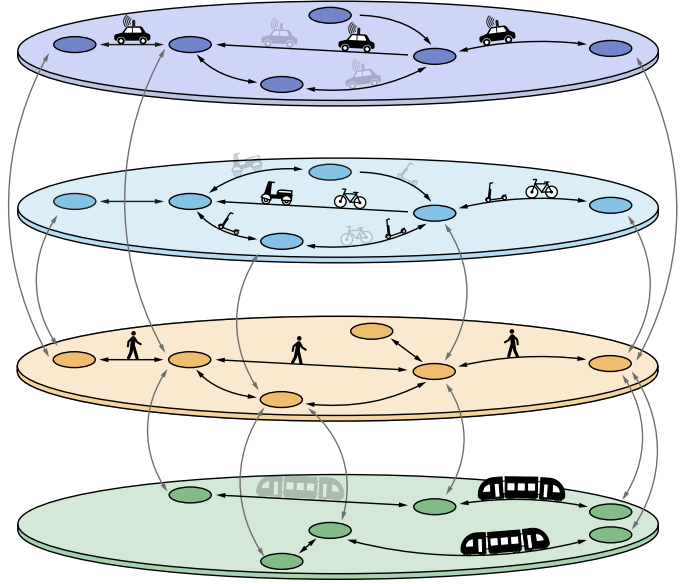


Fig. 2: The intermodal AMoD network consists of road (AVs and μ MVs), public transportation, and walking digraphs. The labeled circles represent stops or intersections and the black arrows denote road links, public transit arcs, or pedestrian pathways. The grey arrows represent the mode-switching arcs connecting them.

with metrics $c: \mathcal{A} \rightarrow \mathcal{S}$. Specifically, $c_{ij} := c\langle i, j \rangle \in \mathcal{S}$ are the metrics associated to arc $\langle i, j \rangle \in \mathcal{A}$. Metrics of interest include edge length, travel time, energy consumption properties, and congestion models. \mathcal{G} is composed of four layers: The road network layer $\mathcal{G}_R = \langle \mathcal{V}_R, \mathcal{A}_R, c_R \rangle$, consisting of an AVs layer $\mathcal{G}_{R,V} = \langle \mathcal{V}_{R,V}, \mathcal{A}_{R,V}, c_{R,V} \rangle$ and a μ MVs layer $\mathcal{G}_{R,M} = \langle \mathcal{V}_{R,M}, \mathcal{A}_{R,M}, c_{R,M} \rangle$, the public transportation layer $\mathcal{G}_P = \langle \mathcal{V}_P, \mathcal{A}_P, c_P \rangle$, and a walking layer $\mathcal{G}_W = \langle \mathcal{V}_W, \mathcal{A}_W, c_W \rangle$. The AVs and the μ MVs networks are characterized by intersections $i \in \mathcal{V}_{R,V}$, $i \in \mathcal{V}_{R,M}$ and road segments $\langle i, j \rangle \in \mathcal{A}_{R,V}$, $\langle i, j \rangle \in \mathcal{A}_{R,M}$, respectively. Similarly, public transportation lines are modeled through station nodes $i \in \mathcal{V}_P$ and line segments $\langle i, j \rangle \in \mathcal{A}_P$. The walking network describes walkable streets $\langle i, j \rangle \in \mathcal{A}_W$, connecting intersections $i \in \mathcal{V}_W$. Mode-switching arcs are modeled as

$$\mathcal{A}_C \subseteq \mathcal{V}_{R,V} \times \mathcal{V}_W \cup \mathcal{V}_W \times \mathcal{V}_{R,V} \cup \mathcal{V}_{R,M} \times \mathcal{V}_W \cup \mathcal{V}_W \times \mathcal{V}_{R,M} \cup \mathcal{V}_P \times \mathcal{V}_W \cup \mathcal{V}_W \times \mathcal{V}_P,$$

connecting the AVs, the μ MVs, and the public transportation layers to the walking layer. To these arcs, we associate metrics c_C .

Consequently, $\mathcal{V} = \mathcal{V}_W \cup \mathcal{V}_{R,V} \cup \mathcal{V}_{R,M} \cup \mathcal{V}_P$ and $\mathcal{A} = \mathcal{A}_W \cup \mathcal{A}_{R,V} \cup \mathcal{A}_{R,M} \cup \mathcal{A}_P \cup \mathcal{A}_C$. Consistently with structural properties of transportation networks in urban environments, we assume \mathcal{G} to be strongly connected.

We now characterize the partial order of edge labeled graphs, which will be instrumental when modeling the MDPI of the mobility system. To do so, we first need to define a partial order on functions.

Definition III.1 (Poset of functions). Consider posets A, B , and consider the set of functions $A \rightarrow B$, denoted by B^A . Given any two functions $f, g: A \rightarrow B$, we define

$$f \preceq_{B^A} g \Leftrightarrow f(a) \preceq_B G(a), \quad \forall a \in A.$$

Lemma III.2. *Definition III.1 defines a poset.*

Definition III.1 allows one to define a poset of edge-labeled multigraphs.

Definition III.3 (Poset of edge-labeled multigraphs). Consider the set of edge-labeled multigraphs, denoted by \mathbf{G} . Given $\mathcal{G}_1, \mathcal{G}_2 \in \mathbf{G}$, with $\mathcal{G}_1 = \langle \mathcal{V}_1, \mathcal{A}_1, c_1 \rangle$, $\mathcal{G}_2 = \langle \mathcal{V}_2, \mathcal{A}_2, c_2 \rangle$, $c_1: \mathcal{A}_1 \rightarrow C$, $c_2: \mathcal{A}_2 \rightarrow C$ we define the order:

$$\mathcal{G}_1 \preceq_{\mathbf{G}} \mathcal{G}_2 \Leftrightarrow (\mathcal{V}_1 \subseteq \mathcal{V}_2) \wedge (\mathcal{A}_1 \subseteq \mathcal{A}_2) \wedge (c_1 \succeq_{C^{\mathcal{A}_1}} c_2|_{\mathcal{A}_1}),$$

where $c_2|_{\mathcal{A}_1}$ is the restriction of c_2 onto the domain of c_1 .

Intuitively, a labeled multigraph dominates another if it includes its nodes and edges, and if the labels are dominating.

Lemma III.4. *Definition III.3 defines a poset.*

We represent customer movements by means of travel requests. A travel request refers to a customer flow starting its trip at a node $o \in \mathcal{V}$ and ending it at a node $d \in \mathcal{V}$.

Definition III.5 (Travel demand). A *travel demand* q is a triple $\langle o, d, \alpha \rangle \in \mathcal{V} \times \mathcal{V} \times \mathbb{R}_+$, described by an origin node $o \in \mathcal{V}$, a destination node $d \in \mathcal{V}$, and the request rate $\alpha > 0$ (i.e., the number of customers who want to travel from o to d per unit time).

Without loss of generality, we can assume that in a set of requests origin-destination pairs are not repeated, and denote the set of all possible set of requests $\mathcal{Q} \subset \mathcal{P}(\mathcal{V} \times \mathcal{V} \times \overline{\mathbb{R}}_{\geq 0})$. This set can be ordered as follows.

Definition III.6 (Poset of travel demand). Consider the set of sets of travel requests \mathcal{Q} . Given any $Q_1, Q_2 \in \mathcal{Q}$, one has:

$$Q_1 := \{ \langle o_i^1, d_i^1, \alpha_i^1 \rangle \}_{i=1}^{M_1} \preceq_{\mathcal{Q}} \{ \langle o_i^2, d_i^2, \alpha_i^2 \rangle \}_{i=1}^{M_2} =: Q_2$$

iff for all $\langle o^1, d^1, \alpha^1 \rangle \in Q_1$ there is some $\langle o^2, d^2, \alpha^2 \rangle \in Q_2$ with $o^1 = o^2$, $d^1 = d^2$, and $\alpha_i^2 \geq \alpha_i^1$. In other words, $Q_1 \preceq_{\mathcal{Q}} Q_2$ if every travel request in Q_1 is in Q_2 as well.

Lemma III.7. *Definition III.6 defines a poset.*

To ensure that a customer is not biased to use a given transportation mode, we assume all requests to appear on the walking digraph, i.e., $o_m, d_m \in \mathcal{V}_W$ for all $m \in \mathcal{M} := \{1, \dots, M\}$. The flow $f_m(i, j) \geq 0$ describes the number of customers per unit time traveling on arc $\langle i, j \rangle \in \mathcal{A}$ and satisfying a travel request m . Furthermore, $f_{0, \mathcal{V}}(i, j) \geq 0$ and $f_{0, \mathcal{M}}(i, j) \geq 0$ denote the flow of empty AVs and μ MVs on AVs arcs $\langle i, j \rangle \in \mathcal{A}_{R, \mathcal{V}}$ and μ MVs arcs $\langle i, j \rangle \in \mathcal{A}_{R, \mathcal{M}}$, respectively. This accounts for rebalancing flows of AVs and μ MVs between a customer's drop-off and the next customer's pick-up. Assuming AVs and μ MVs to carry one customer at a time, the flows satisfy

$$\sum_{i: \langle i, j \rangle \in \mathcal{A}} f_m(i, j) + \mathbb{1}_{j=o_m} \cdot \alpha_m = \sum_{k: \langle j, k \rangle \in \mathcal{A}} f_m(j, k) + \mathbb{1}_{j=d_m} \cdot \alpha_m \quad \forall m \in \mathcal{M}, j \in \mathcal{V} \quad (1a)$$

$$\sum_{i: \langle i, j \rangle \in \mathcal{A}_{R, \mathcal{V}}} f_{\text{tot}, \mathcal{V}}(i, j) = \sum_{k: \langle j, k \rangle \in \mathcal{A}_{R, \mathcal{V}}} f_{\text{tot}, \mathcal{V}}(j, k) \quad \forall j \in \mathcal{A}_{R, \mathcal{V}} \quad (1b)$$

$$\sum_{i: \langle i, j \rangle \in \mathcal{A}_{R, \mathcal{M}}} f_{\text{tot}, \mathcal{M}}(i, j) = \sum_{k: \langle j, k \rangle \in \mathcal{A}_{R, \mathcal{M}}} f_{\text{tot}, \mathcal{M}}(j, k) \quad \forall j \in \mathcal{A}_{R, \mathcal{M}}, \quad (1c)$$

where $\mathbb{1}_{j=x}$ denotes the boolean indicator function, $f_{\text{tot}, \mathcal{V}}(i, j) := f_{0, \mathcal{V}}(i, j) + \sum_{m \in \mathcal{M}} f_m(i, j)$, and $f_{\text{tot}, \mathcal{M}}(i, j) := f_{0, \mathcal{M}}(i, j) + \sum_{m \in \mathcal{M}} f_m(i, j)$. Specifically, (1a) guarantees flows conservation for every transportation demand, (1b) preserves flow conservation for AVs on every road node, and (1c) preserves flow conservation for μ MVs on every road node. Combining conservation of customers (1a) with the conservation of AVs (1b) and μ MVs (1c) guarantees rebalancing AVs and μ MVs to match the demand.

B. Labeling Graphs with Relevant Attributes

In the following, we specify how to label the graphs composing the full mobility network. Specifically, edge-labeling maps will be of the form $c: \mathcal{A} \rightarrow \mathcal{S}$, where $\mathcal{S} = \mathbb{R}_{\geq 0}^5$ represents link length, time needed to traverse it, its speed limit, related emissions, and capacity.

1) *Walking arcs*: We infer arc lengths s_{ij} from geographical data and, assuming constant walking speed v_W , travel time results from $t_{ij} = s_{ij}/v_W$. As speeds limits, congestion, and energy consumption do not apply to walking graphs, we set $v_{L, ij} = \infty, k_{ij} = \infty, e_{ij} = 0$. Accordingly,

$$c_W: \mathcal{A}_W \rightarrow \mathcal{S} \\ \langle i, j \rangle \mapsto \langle s_{ij}, t_{ij}, v_{L, ij}, e_{ij}, k_{ij} \rangle.$$

2) *Public transit arcs*: We infer arc lengths s_{ij} from public transit network data. Furthermore, assuming that the public transportation system at node j operates with the frequency φ_j , travel time results from $t_{ij} = t_{ij}^{\text{nom}} + t_{WS} + 1/(2\varphi_j)$, where t_{ij}^{nom} is the in-vehicle travel time (inferred from public transit schedules) and t_{WS} is a constant sidewalk-to-station travel time. We ignore capacity and speed limits, so that $k_{ij} = v_{L, ij} = \infty$. For the public transportation system we assume a constant energy consumption per unit time. This approximation is reasonable in urban environments, where the operation of the public transportation system is independent from the number of customer serviced, and its energy consumption is therefore invariant. Therefore, we write $e_{ij} = \kappa t_{ij}$, $\kappa > 0$. Accordingly,

$$c_P: \mathcal{A}_P \rightarrow \mathcal{S} \\ \langle i, j \rangle \mapsto \langle s_{ij}, t_{ij}, v_{L, ij}, e_{ij}, k_{ij} \rangle.$$

3) *Road arcs for AVs*: Each road arc is characterized by a length s_{ij} , a speed limit $v_{L, ij}$, and a capacity k_{ij} , all derived from road network data. We consider AVs driving at speed v_V , so that travel time reads

$$t_{ij} = \frac{s_{ij}}{\min\{v_V, v_{L, ij}\}}.$$

We compute the energy consumption of AVs via an urban driving cycle. In particular, the cycle is scaled so that its

average speed $v_{\text{avg,cycle}}$ matches the free-flow speed on the link. The energy consumption of road link $\langle i, j \rangle$ is scaled as

$$e_{ij} = e_{\text{cycle}} \cdot \frac{s_{ij}}{s_{\text{cycle}}}.$$

Collectively,

$$c_{R,V}: \mathcal{A}_{R,V} \rightarrow \mathcal{S} \\ \langle i, j \rangle \mapsto \langle s_{ij}, t_{ij}, v_{L,ij}, e_{ij}, k_{ij} \rangle.$$

4) *Road arcs for μ MVs*: Each road arc is characterized by a length s_{ij} and a speed limit $v_{L,ij}$, derived from road network data, while we neglect arc capacity (i.e., $k_{ij} = \infty$). Assuming μ MVs driving at speed v_M , travel time reads

$$t_{ij} = \frac{s_{ij}}{\min\{v_M, v_{L,ij}\}}.$$

For μ MVs we consider a distance-based energy consumption, i.e. $e_{ij} = \iota s_{ij}$, with $\iota > 0$. Overall,

$$c_{R,M}: \mathcal{A}_{R,M} \rightarrow \mathcal{S} \\ \langle i, j \rangle \mapsto \langle s_{ij}, t_{ij}, v_{L,ij}, e_{ij}, k_{ij} \rangle.$$

5) *Transfer arcs*: We define travel time t_{ij} as follows: we assume that the average waiting time for AVs is t_{WV} , the average time needed to reach a μ MV is t_{WM} , and switching from the AVs graph, the μ MVs graph, and the public transit graph to the pedestrian graph takes the transfer times t_{VW} , t_{MW} , and t_{SW} , respectively. For each arc, we set length and energy consumption to zero (i.e., $s_{ij} = e_{ij} = 0$) and ignore capacity and speed limit (i.e., $k_{ij} = v_{L,ij} = \infty$). Overall,

$$c_C: \mathcal{A}_C \rightarrow \mathcal{S} \\ \langle i, j \rangle \mapsto \langle s_{ij}, t_{ij}, v_{L,ij}, e_{ij}, k_{ij} \rangle.$$

C. Road Congestion

We assume that road arcs are subject to a normalized capacity k_{ij} , which could arise from the difference of the nominal road capacity and the exogenous road usage:

$$f_{\text{tot},V}(i, j) \leq k_{ij}. \quad (2)$$

We assume that the central authority operates the AMoD fleet such that vehicles travel at free-flow speed throughout the road network of the city, meaning that the total flow on each road link must be below the link's capacity. Therefore, we capture congestion effects with the threshold model. Finally, we assume μ M to not significantly contribute to congestion [43].

D. Discussion

First, the demand is assumed to be time-invariant and flows are allowed to have fractional values. This assumption is in line with the mesoscopic and system-level planning perspective of our study. Second, we model congestion effects using a threshold model. This approach can be interpreted as a municipality preventing mobility solutions to exceed the critical flow density on road arcs. AVs and μ MVs can therefore be assumed to travel at free flow speed [44]. This assumption is realistic for an initial low penetration of new mobility systems in the transportation market, especially when the AV and μ MV fleets are limited in size. Finally, we allow AVs and μ MVs to transport one customer at a time [45].

E. Co-Design Framework

We integrate the intermodal framework presented in Section III-A in the co-design formalism, allowing the decoupling of the CDPI of a complex system in the MDPIs of its individual components in a modular, compositional, and systematic fashion. To achieve this, we decouple the CDPI in the MDPIs of the individual AV (Section III-E1), the AVs fleet (Sections III-E4 to III-E6), the individual μ MV (Section III-E2), the μ MVs fleet (Sections III-E4 to III-E6), and the public transportation system (Section III-E3). Their interconnection is presented in Sections III-E7 to III-E9, where we propose multiple model versions, showcasing the flexibility of the developed framework. We aim at computing the antichain of resources, quantified in terms of costs, average travel time per trip, and emissions required to provide the mobility service to a set of customers. For each model, we provide descriptions and formal proofs of integration in the co-design framework.

1) *The AV MDPI*: The AV MDPI selects the labeled graph on which the AV provider wants to operate. The selection happens via the choice of the achievable speed of the AVs as follows. AVs safety protocols impose a maximum achievable velocity v_V . Furthermore, in order to prevent too slow and therefore dangerous driving behaviors [46], we only consider AVs arcs through which the AVs can drive at least at a fraction β of the speed limit. Specifically, AVs can drive on arc $\langle i, j \rangle \in \mathcal{A}_{R,V}$ if and only if

$$v_V \geq \beta \cdot \pi_{v_L} c_{R,V}(i, j), \quad (3)$$

where $\beta \in (0, 1]$, and π_{v_L} projects the part of $c_{R,V}(i, j)$ related to v_L . The elimination of forbidden arcs given an achievable speed can be achieved through the following map (mnemonics for reduction):

$$\text{red}_{R,V}: \mathbb{R}_{\geq 0} \rightarrow \langle \mathbf{G}, \leq_{\mathbf{G}} \rangle \\ v_V \mapsto \langle \mathcal{V}_{R,V}, \mathcal{A}, c \rangle,$$

where

$$\mathcal{A} = \{a \in \mathcal{A}_{R,V} : \text{Equation (3) holds}\}, \\ c = \langle \pi_s c_{R,V}, \frac{\pi_s c_{R,V}}{\min\{v_V, \pi_{v_L} c_{R,V}\}}, \pi_{v_L} c_{R,V}, \pi_e c_{R,V}, \pi_k c_{R,V} \rangle. \quad (4)$$

Lemma III.8. *The map $\text{red}_{R,V}$ is monotone.*

Under the rationale that driving safely at higher speed requires more advanced sensing and algorithmic capabilities [7], we model the achievable speed of the AVs v_V as a *monotone* function of the vehicle fixed costs $C_{V,f}$ (resulting from the cost of the vehicle $C_{V,v}$ and the cost of its automation $C_{V,a}$) and the mileage-dependent operational costs $C_{V,o}$ (accounting for maintenance, cleaning, energy consumption, depreciation, and opportunity costs [47]).

MDPI Definition: The AV MDPI, denoted d_{AV} , provides the functionality $\mathcal{G}_{AV} \in \mathbf{G}$ (i.e., the functionality of servicing a specific network with a specific performance) and requires the resources $C_{V,f}, C_{V,o} \in \mathbb{R}_{\geq 0}$. The implementations space \mathcal{I}_{AV} consists of models of the AVs. Formally: $d_{AV}: \mathbf{G} \dashrightarrow \mathbb{R}_{\geq 0}^2$.

Lemma III.9. *d_{AV} is a well-defined MDPI.*

2) *The μ MV MDPI*: The μ M MDPI comprises the selection of the labeled graph on which to operate, again resumed in the maximal speed achievable by μ MVs. Given an achievable speed v_M , one obtains the resulting graph as follows:

$$\text{red}_{R,M}: \mathbb{R}_{\geq 0} \rightarrow \langle \mathbf{G}, \preceq_{\mathbf{G}} \rangle \\ v_M \mapsto \langle \mathcal{V}_{R,M}, \mathcal{A}_{R,M}, c \rangle,$$

where

$$c = \langle \pi_s c_{R,M}, \frac{\pi_s c_{R,M}}{\min\{v_M, \pi_{v_L} c_{R,M}\}}, \pi_{v_L} c_{R,M}, \pi_e c_{R,M}, \pi_k c_{R,M} \rangle.$$

Lemma III.10. *The map $\text{red}_{R,M}$ is monotone.*

Following the rationale that different μ MVs can reach different speeds and have different prices, we model the achievable speed of the μ MV v_M as a *monotone* function of the μ MV fixed costs $C_{M,f}$ and the mileage-dependent operational costs $C_{M,o}$.

MDPI Definition: Therefore, the μ M MDPI, denoted d_{MM} , provides the functionality $\mathcal{G}_{MM} \in \mathbf{G}$ (i.e., the functionality of servicing a specific network with a specific performance) and requires the resources $C_{M,f}, C_{M,o} \in \overline{\mathbb{R}}_{\geq 0}$. The implementations space \mathcal{I}_M consists of instances of the μ MVs. Formally: $d_{MM}: \mathbf{G} \mapsto \overline{\mathbb{R}}_{\geq 0}^2$.

Lemma III.11. *d_{MM} is a well-defined MDPI.*

3) *The Subway MDPI*: The public transit MDPI comprises the selection of the labeled network on which to operate, now resumed in the choice of fleet size for the subway system. Specifically, we assume the service frequency φ_j to scale monotonically with the size of the train fleet n_S . In the linear case, one has:

$$\frac{\varphi_j}{\varphi_{j,\text{base}}} = \frac{n_S}{n_{S,\text{base}}},$$

where $\varphi_{j,\text{base}}$ and $n_{S,\text{base}}$ are respective existing baselines. Given a train fleet size, one obtains the resulting network as follows:

$$\text{red}_P: \mathbb{N} \rightarrow \langle \mathbf{G}, \preceq_{\mathbf{G}} \rangle \\ n_S \mapsto \langle \mathcal{V}_P, \mathcal{A}_P, c \rangle,$$

where

$$c = \langle \pi_s c_P, t_{WS} + \frac{n_{S,\text{base}}}{2n_S \varphi_{j,\text{base}}}, \pi_{v_L} c_P, \pi_e c_P, \pi_k c_P \rangle.$$

Lemma III.12. *The map red_P is monotone.*

We relate a train fleet of size n_S to the fixed costs $C_{S,f}$ (accounting for train and infrastructural costs) and to the operational costs $C_{S,o}$ (accounting for energy consumption, vehicles depreciation, and train operators' wages). Given the passengers-independent public transit operation in today's cities, we assume the operational costs $C_{S,o}$ to be mileage independent and to only vary with the size of the fleet. Assuming an average train's life of l_S , and a baseline subway fleet of $n_{S,\text{baseline}}$ trains, costs are

$$C_S = \frac{C_{S,f}}{l_S} \cdot n_{S,a} + C_{S,o}.$$

Moreover, operating a fleet of trains entails the CO₂ emissions

$$m_{\text{CO}_2,S,\text{tot}} = m_{\text{CO}_2,S} \cdot n_S.$$

MDPI Definition: The public transit MDPI, denoted d_P , provides the functionality $\mathcal{G}_P \in \mathbf{G}$ (i.e., the functionality of servicing a specific network with a specific performance) and requires the resources $C_S \in \overline{\mathbb{R}}_{\geq 0}$ and $m_{\text{CO}_2,S,\text{tot}} \in \overline{\mathbb{R}}_{\geq 0}$. The implementations space \mathcal{I}_P consists of different train acquisition choices. Formally: $d_P: \mathbf{G} \mapsto \overline{\mathbb{R}}_{\geq 0}^2$.

Lemma III.13. *d_P is a well-defined MDPI.*

4) *The Intermodal Mobility System MDPI (Version 1)*: The first version of the intermodal mobility system MDPI considers demand satisfaction as a functionality.

To successfully satisfy a given set of travel requests, we require the following resources:

- the mobility network resulting from the design of AVs, AVs $\mathcal{G}_{AV} = \langle \mathcal{V}_{AV}, \mathcal{A}_{AV}, c_{AV} \rangle$,
- the mobility network resulting from the design of public transit $\mathcal{G}_P = \langle \mathcal{V}_P, \mathcal{A}_P, c_P \rangle$,
- the number of available AVs per fleet $n_{V,\text{max}}$,
- the average travel time of a trip

$$t_{\text{avg}} := \frac{1}{\alpha_{\text{tot}}} \sum_{\substack{m \in \mathcal{M}, \\ \langle i,j \rangle \in \mathcal{A}_W \cup \mathcal{A}_{AV} \cup \mathcal{A}_P \cup \mathcal{A}_C}} \pi_t c(i,j) \cdot f_m(i,j),$$

with

$$\alpha_{\text{tot}} := \sum_{m \in \mathcal{M}} \alpha_m, \quad (5)$$

- the total distance driven by the AVs per unit time

$$s_{V,\text{tot}} := \sum_{\langle i,j \rangle \in \mathcal{A}_{AV}} \pi_s c_{AV}(i,j) \cdot f_{\text{tot},V}(i,j), \quad (6)$$

- the total AVs CO₂ emissions per unit time

$$m_{\text{CO}_2,V,\text{tot}} := \gamma \cdot \sum_{\langle i,j \rangle \in \mathcal{A}_{AV}} \pi_e c_{AV} \cdot f_{\text{tot},V}(i,j). \quad (7)$$

We assume that AVs are routed to maximize the customers' welfare, defined without loss of generality as the average travel time t_{avg} . Hence, we link functionality and resources of the mobility system MDPI through the optimization problem:

$$\begin{aligned} & \min_{\substack{\{f_m\}_m \\ f_{0,v}}} t_{\text{avg}} \\ & \text{s.t. Eq.(1),} \\ & \text{Eq.(2) } \forall \langle i,j \rangle \in \mathcal{A}_{AV}, \\ & \sum_{\langle i,j \rangle \in \mathcal{A}_{AV}} f_{\text{tot},V}(i,j) \cdot \pi_t c_{AV}(i,j) \leq n_{V,\text{max}}, \end{aligned} \quad (8)$$

where we express the number of vehicles on arc $\langle i,j \rangle$ as the multiplication of the total vehicles flow on the arc and its travel time.

MDPI Definition: The intermodal mobility system MDPI has as functionality the satisfied requests $Q \in \mathcal{Q}$ and the mentioned resources. Furthermore, \mathcal{I}_O consists of specific intermodal scenarios. Formally: $d_{\text{IAMOD}}: \mathcal{Q} \mapsto \mathbf{G}^2 \times \mathbb{N} \times \overline{\mathbb{R}}_{\geq 0}^3$.

Lemma III.14. *$d_{\text{IAMOD},1}$ is a well-defined MDPI.*

5) *The Intermodal Mobility System MDPI (Version 2)*: The second version of the intermodal mobility system MDPI still considers demand satisfaction as a functionality, now including μM options. To successfully satisfy a given set of travel requests, we require the following resources:

- $\mathcal{G}_{AV} = \langle \mathcal{V}_{AV}, \mathcal{A}_{AV}, c_{AV} \rangle$ as in Section III-E4,
- $\mathcal{G}_P = \langle \mathcal{V}_P, \mathcal{A}_P, c_P \rangle$ as in Section III-E4,
- the mobility network resulting from the design of μMs , $\mu\text{Ms } \mathcal{G}_{MM} = \langle \mathcal{V}_{MM}, \mathcal{A}_{MM}, c_{MM} \rangle$,
- $n_{V,\max}$ as in Section III-E4,
- the number of available μMVs per fleet $n_{M,\max}$,
- the (adapted) average travel time of a trip

$$t_{\text{avg}} := \frac{1}{\alpha_{\text{tot}}} \sum_{\langle i,j \rangle \in \mathcal{A}_W \cup \mathcal{A}_{AV} \cup \mathcal{A}_{MM} \cup \mathcal{A}_P \cup \mathcal{A}_C} \pi_t c(i,j) \cdot f_m(i,j),$$

with α_{tot} as in Equation (5),

- $s_{V,\text{tot}}$ as in Equation (6),
- the total distance driven by the μMVs per unit time

$$s_{M,\text{tot}} := \sum_{\langle i,j \rangle \in \mathcal{A}_{MM}} \pi_s c_{MM}(i,j) \cdot f_{\text{tot},M}(i,j),$$

- $m_{\text{CO}_2,V,\text{tot}}$ as in Equation (7),
- the total μMVs CO_2 emissions per unit time

$$m_{\text{CO}_2,M,\text{tot}} := \gamma \cdot \sum_{\langle i,j \rangle \in \mathcal{A}_{MM}} \pi_e c_{MM} \cdot f_{\text{tot},M}(i,j),$$

where γ relates energy consumption and CO_2 emissions.

We assume that AVs and μMVs are routed to maximize the customers' welfare, defined without loss of generality as the average travel time t_{avg} . Hence, we link functionality and resources of the mobility system MDPI through the following optimization problem, extending Equation (8):

$$\begin{aligned} & \min_{\substack{\{f_m\}_m \\ f_{0,V} \\ f_{0,M}}} t_{\text{avg}} \\ & \text{s.t. Eq.(1),} \\ & \text{Eq.(2) } \forall \langle i,j \rangle \in \mathcal{A}_{AV}, \\ & \sum_{\langle i,j \rangle \in \mathcal{A}_{AV}} f_{\text{tot},V}(i,j) \cdot \pi_t c_{AV}(i,j) \leq n_{V,\max}, \\ & \sum_{\langle i,j \rangle \in \mathcal{A}_{MM}} f_{\text{tot},M}(i,j) \cdot \pi_t c_{MM}(i,j) \leq n_{M,\max}, \end{aligned} \quad (9)$$

where we express the number of vehicles on arc $\langle i,j \rangle$ as the multiplication of the total vehicles flow on the arc and its travel time.

MDPI Definition: The intermodal mobility system MDPI has as functionality $\mathcal{Q} \in \mathcal{Q}$ and the mentioned resources. Furthermore, \mathcal{I}_O consists of specific intermodal scenarios. Formally: $d_{\text{IAMOD},2}: \mathcal{Q} \mapsto \mathbf{G}^3 \times \mathbb{N}^2 \times \mathbb{R}_{\geq 0}^5$.

Lemma III.15. $d_{\text{IAMOD},2}$ is a well-defined MDPI.

6) *The Intermodal Mobility System MDPI (Version 3)*: We extend the setting presented in Section III-E4 by including a new functionality. Specifically, the intermodal mobility system MDPI not only provides demand satisfaction as a functionality,

but also provides the revenue ρ arising from the mobility offer, which reads:

$$\rho = p_{AV} s_{V,\text{tot}} + p_P \sum_{\langle i,j \rangle \in \mathcal{A}_C \cap \mathcal{V}_W \times \mathcal{V}_P} f_m(i,j),$$

where p_{AV} is a distance-based price to use AVs and p_P is a fixed entry price for the subway system. Accordingly, we modify the optimization problem to account for both average travel time and average cost of fare:

$$\begin{aligned} & \min_{\substack{\{f_m\}_m \\ f_{0,V}}} V_T t_{\text{avg}} + \frac{1}{\alpha_{\text{tot}}} \rho \\ & \text{s.t. Eq.(1),} \\ & \text{Eq.(2) } \forall \langle i,j \rangle \in \mathcal{A}_{AV}, \\ & \sum_{\langle i,j \rangle \in \mathcal{A}_{AV}} f_{\text{tot},V}(i,j) \cdot \pi_t c_{AV}(i,j) \leq n_{V,\max}, \end{aligned} \quad (10)$$

where V_T is the value of time.

MDPI Definition: This new version of the intermodal mobility system MDPI has as functionality the satisfied requests $\mathcal{Q} \in \mathcal{Q}$ and the total revenue $\rho \in \overline{\mathbb{R}}_{\geq 0}$ and the mentioned resources. Furthermore, \mathcal{I}_O consists of specific intermodal scenarios (including specific price choices). Formally: $d_{\text{IAMOD},3}: \mathcal{Q} \times \overline{\mathbb{R}}_{\geq 0} \mapsto \mathbf{G}^2 \times \mathbb{N} \times \overline{\mathbb{R}}_{\geq 0}^3$.

Lemma III.16. $d_{\text{IAMOD},3}$ is a well-defined MDPI.

7) *The Mobility MDPI (Version 1)*: The functionality of the system is to satisfy the customers' demand. Formally, the functionality provided by the CDPI is the set of travel requests and coincides with the functionalities of d_{I_1} . To provide the mobility service, three resources are required. First, on the customers' side, we require the average travel time defined in Section III-E4. Second, on the side of the central authority, the resource is the total transportation cost of the intermodal mobility system. Assuming an average AV's life of l_V , an average μMV 's life of l_M , we express the total costs as

$$C_{\text{tot}} = C_V + C_S,$$

where C_V is the AVs-related cost

$$C_V = \frac{C_{V,f}}{l_V} \cdot n_{V,\max} + C_{V,o} \cdot s_{V,\text{tot}},$$

and C_S is the public transit-related cost. Third, on the environmental side, we consider the total CO_2 emissions

$$m_{\text{CO}_2,\text{tot}} = m_{\text{CO}_2,V,\text{tot}} + m_{\text{CO}_2,S,\text{tot}}.$$

MDPI definition: Formally: $d_{\text{Mob}_1}: \mathcal{Q} \mapsto \overline{\mathbb{R}}_{\geq 0}^3$. The MDPI formal diagram is reported in Figure 3a.

Lemma III.17. d_{Mob_1} is a well-defined MDPI.

8) *The Mobility MDPI (Version 2)*: As in Section III-E7, the functionality provided by the MDPI is the set of travel requests. To provide the mobility service, three resources are required. First, on the customers' side, we require an average travel time, defined in (III-E5). Second, on the side of the central authority, the resource is the total transportation cost of the intermodal mobility system. To the cost defined in

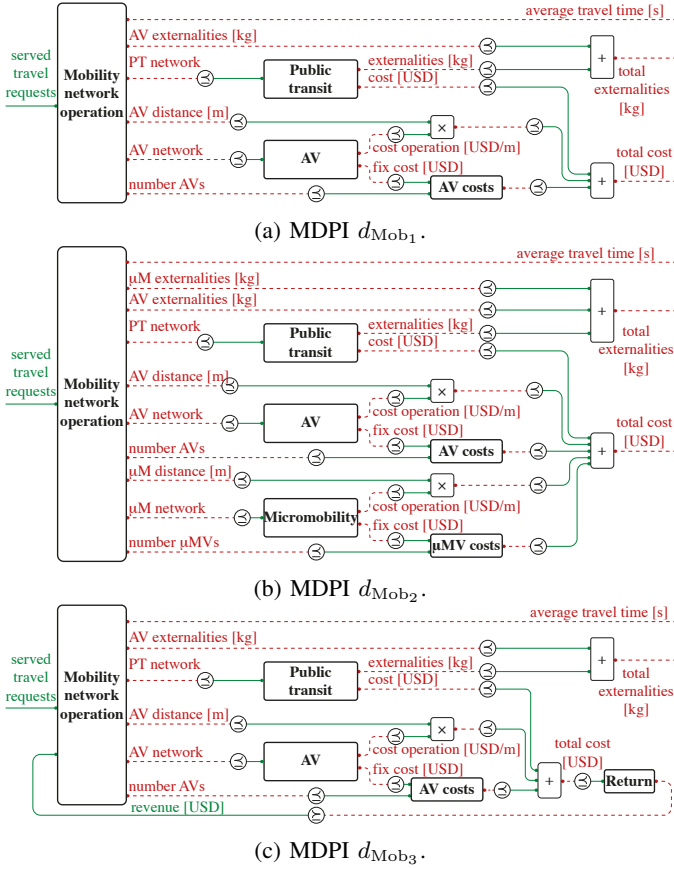


Fig. 3: Co-design diagrams for the MDPIs defined in Section III-E.

Section III-E8, we add the cost related to μM . Assuming an average μMV 's life of l_M we get

$$C_{\text{tot}} = C_V + C_M + C_S,$$

where C_M is the μMV -related cost

$$C_M = \frac{C_{M,f}}{l_M} \cdot n_{M,\text{max}} + C_{M,o} \cdot s_{M,\text{tot}},$$

Third, we add the μM -related emissions to the ones computed in Section III-E7:

$$m_{\text{CO}_2,\text{tot}} = m_{\text{CO}_2,V,\text{tot}} + m_{\text{CO}_2,M,\text{tot}} + m_{\text{CO}_2,S,\text{tot}}.$$

MDPI definition: Formally: $d_{\text{Mob}_2}: \mathcal{Q} \mapsto \overline{\mathbb{R}}_{\geq 0}^3$. The MDPI is reported in Figure 3b.

Lemma III.18. d_{Mob_2} is a well-defined MDPI.

9) *The Mobility MDPI (Version 3):* We now extend the setting presented in Section III-E7 by including the structure presented in Section III-E6. Specifically, the functionality provided by the MDPI coincides with the functionalities of d_{13} (i.e., includes travel requests and total revenue). Furthermore, to provide the functionalities the three resources introduced in Section III-E7 are required: t_{avg} , C_{tot} , and $m_{\text{CO}_2,\text{tot}}$. We introduce a feedback loop, by requiring the total revenue ρ to at least cover a fraction χ of the total costs, i.e., $\rho \geq \chi \cdot C_{\text{tot}}$.

MDPI definition: Formally: $d_{\text{Mob}_3}: \mathcal{Q} \mapsto \overline{\mathbb{R}}_{\geq 0}^2$. The MDPI is reported in Figure 3c.

Lemma III.19. d_{Mob_3} is a well-defined MDPI.

10) *Discussion:* First, we lump the AV's autonomy in its achievable velocity. We leave to future research more elaborated and realistic AV models, accounting, for instance, for accidents rates [48] and for safety levels. For the latter, we plan on explicitly including the autonomy model, as in [7]. Similarly, the ability of μM to operate on specific network links is a regulatory aspect, which depends on factors not related to vehicle design. Second, we assume the service frequency of the subway system to scale monotonically with the number of trains. We inherently assume that the existing infrastructure can homogeneously accommodate the acquired train cars. To justify the assumption, we include an upper bound on the number of potentially acquirable trains in our case study design in Section IV. Nonetheless, the co-design framework can also accommodate more sophisticated frequency models. Third, we highlight that the intermodal mobility framework is only one of the many feasible ways to map total demand to travel time, costs, and emissions. Specifically, practitioners can easily replace the corresponding MDPI (here specified via a multi-commodity flow model and an optimization problem) with different models (e.g., MATSim [49]), as long as the light condition of monotonicity of the MDPI is preserved. In this sense, the framework is user-friendly, allowing users to plug in different models and analyze the results. In our setting, we conjecture customers and vehicles routes to be centrally controlled by the central authority in a socially-optimal fashion. Here, investment costs have to be covered by the central authority. We leave more complex cost analysis, and the study of strategic interactions of stakeholders, to future studies. Fourth, we assume a homogeneous fleet of AVs and μMVs . Nevertheless, our model is readily extendable to capture heterogeneous fleets. Finally, we consider a fixed travel demand, and compute the antichain of resources providing it. Nonetheless, our formalization can be easily extended to arbitrary demand models preserving the monotonicity of the CDPI to account, for instance, for elastic effects [50], [51].

IV. DESIGN OF EXPERIMENTS AND RESULTS

In this section, we showcase the co-design framework presented in Section III on the case of Washington D.C., USA, leveraging real mobility data. We detail our experimental design in Section IV-A and present numerical results in Section IV-B.

A. Design of Experiments

Our example study is based on the urban area of Washington D.C., USA. The city road network and its features are imported from OpenStreetMap [52], whilst the public transit network together with its schedules are extracted from GTFS [53]. Original demand data is obtained by merging origin-destination pairs of the morning peak of Monday 1st May, 2017, provided by taxi companies [54] and the Washington Metropolitan Area Transit Authority (WMATA) [55]. On the public transportation side, we focus our studies on

the MetroRail system and its design. To take account of the recently increased presence of ride-hailing companies, the taxi demand rate is scaled by a factor of 5 [56]. The complete demand dataset includes 16,430 distinct origin-destination pairs, describing travel requests. To account for congestion effects, the nominal road capacity is computed as in [57] and an average baseline usage of 93% is assumed, in line with [58]. We assume an AV fleet composed of battery electric BEV-250 mile AVs [59]. We summarize the main parameters characterizing our case studies together with their bibliographic sources in Table I. In the remainder of this section, we solve the co-design problem presented in Section III². The diagrams we reported represent the “skeleton” of the design hierarchy. In order to fill the blocks, one needs feasibility relations, which have been described in previous sections. Note that the proposed approach is extremely flexible, since it allows one to specify feasibility relations via catalogues (e.g., for vehicle models), formulas (e.g., for the cost structures), and simulation/optimization problems (e.g., for the intermodal mobility system). Once one identifies the MDPIs, one can directly use the PyMCDP solver [60]. The solver provides the full set of optimal solutions. If it converges to an empty set, the solution corresponds to a certificate of infeasibility. Beside our basic setting (S1), we evaluate the sensitivity of the design strategies to different models of automation costs of AVs (S2–S4) assess the impact of emerging μ M solutions, showing how one can easily include new modes of transportation in the framework (S5), and investigate pricing strategies in (S6). We summarize the considered mobility solutions and their complementarity in Table II.

S1 - Basic setting: We consider the co-design of the mobility system by means of AMoD and public transportation systems (Section III-E7), and do not include μ M solutions (cf. S5). Specifically, we co-design the system by means of the AV fleet size, achievable free-flow speed (see Lemma III.8), and subway service frequency (see Lemma III.12): The municipality is allowed to (i) deploy an AV fleet of size $n_{V,\max} \in \{0, 500, 1,000, \dots, 5,000\}$ vehicles, (ii) choose the single AV achievable speed (determining the serviced mobility network) $v_V \in \{20 \text{ mph}, 25 \text{ mph}, \dots, 50 \text{ mph}\}$, and (iii) increase the subway service frequency φ_j by a factor of 0%, 50%, or 100%. In line with recent literature [61]–[65], [77], we assume an average achievable-velocity-independent cost of automation.

S2 - Speed-dependent automation costs: To relax the potentially unrealistic assumption of a velocity-independent automation cost, we consider a performance-dependent cost structure, detailed in Table I. The large variance in sensing technologies available on the market and their performances suggests that AV costs are, in fact, performance-dependent [7], [78]. Indeed, the technology currently required to safely operate an autonomous vehicle at 50 mph is substantially more sophisticated, and therefore more expensive, than the one needed at 20 mph.

²The solution techniques for this kind of optimization problems and their complexity are described in [3, Proposition 5], in the appendix, and in our talk at <https://bit.ly/3e1IO6f>. We are writing books on the subject, and teaching classes; see <https://applied-compositional-thinking.engineering>.

Furthermore, the frenetic evolution of automation techniques will inevitably reduce automation costs: Experts forecast a massive automation cost reduction (up to 90%) in the next decade, principally due to mass-production of AVs sensing technology [79], [80]. Therefore, we perform our studies with current (2022) automation costs as well as with their projections for the upcoming years (2025) [59], [77], [80].

S3 - High automation costs: We assess the impact of high automation costs. In particular, we assume a performance-independent automation cost of 0.5 Mil USD/car, capturing the extremely high research and development costs that AVs companies are facing today [81], as well as insurance costs and infrastructural investments. The latter, often referred to as “autonomy-enabling infrastructure”, would allow high driving speeds, and could consist of dedicated roads, equipped with sensors and cloud computing capabilities, enhancing the performance of AVs.

S4 - MoD setting: We analyze the current Mobility-on-Demand (MoD) case. The cost structure of MoD systems is characterized by lower vehicle costs (due to lack of automation) and higher operation costs, mainly due to drivers’ salaries.

S5 - Impact of new transportation modes: We show the modularity of our framework by evaluating the impact of μ M solutions on urban mobility (Section III-E8). We consider ESs (e.g., Lime in DC), SBs (e.g., Capital Bikeshare in DC), Ms (e.g., Revel in DC), and FCMs. In addition to the design parameters introduced in the basic setting, we design the specific μ M solution $M \in \{\text{ES,SB,M,FCM}\}$ and the μ M fleet size $n_{M,\max} \in \{0, 500, 1,000, \dots, 5,000\}$ vehicles (see Lemma III.10). We study the joint deployment of μ M solutions and AVs, and therefore consider the extended settings of 2022 and 2025.

S6 - Pricing: We show another extension of our framework to capture pricing strategies and infrastructure-contributing revenues (Section III-E9) in the 2022 setting. We consider AMoD service providers that choose from an exemplary set of prices $\{0.8, 1.2, 1.6, 2.4, 3.2\}$ (expressed in USD/mile) and public transit authorities choosing fare prices from the set $\{1.0, 2.0, 4.0, 6.0\}$ (expressed in USD per ride). Furthermore, we consider a municipality willing to cover 50% (just a particular choice) of the investment cost through the revenues of mobility services. (i.e., the revenue gained from travelers paying for the trips should at least be enough to cover 50% of the investment costs).

B. Results

1) *Basic setting:* Figure 4a reports the solution of the co-design problem through the antichain consisting of the total CO₂ emissions, average travel time, and total transportation cost. The design solutions are *rational* (and not comparable), since there exists no instance which simultaneously yields lower emissions, average travel time, and cost. In the interest of clarity, we prefer a two-dimensional antichain representation, where emissions are included in the costs via a conver-

³The description in this caption is valid for all the following figures.

Parameter	Variable	Value								Units	Source
Road usage	u_{ij}	93								%	[58]
		S1	S2 (2022)	S2 (2025)	S3	S4	S5 (2022)	S5 (2025), S6			
AVs operational cost	$C_{V,o}$	0.084	0.084	0.062	0.084	0.50	0.084	0.062	USD/mile	[59], [61]	
Vehicle cost	C_V	32	32	26	32	32	32	26	kUSD/car	[59]	
	20 mph	15	20	3.7	500	0	20	3.7	kUSD/car	[61]–[65]	
	25 mph	15	30	4.4	500	0	300	4.4	kUSD/car	[61]–[65]	
	30 mph	15	55	6.2	500	0	55	6.2	kUSD/car	[61]–[65]	
AV automation cost	$C_{V,a}$	15	90	8.7	500	0	90	8.7	kUSD/car	[61]–[65]	
	35 mph	15	115	9.8	500	0	115	9.8	kUSD/car	[61]–[65]	
	40 mph	15	130	12	500	0	130	12	kUSD/car	[61]–[65]	
	45 mph	15	150	13	500	0	150	13	kUSD/car	[61]–[65]	
AV life	t_V	5	5	5	5	5	5	5	year	[59]	
CO ₂ per Joule	γ	0.14	0.14	0.14	0.14	0.14	0.14	0.14	g/kJ	[66]	
Time \mathcal{G}_W to $\mathcal{G}_{R,V}$	t_{WV}	300	300	300	300	300	300	300	s	-	
Time $\mathcal{G}_{R,V}$ to \mathcal{G}_W	t_{VW}	60	60	60	60	60	60	60	s	-	
Speed limit fraction	β	1/1.3	1/1.3	1/1.3	1/1.3	1/1.3	1/1.3	1/1.3	-	[46]	
		ES	SB	M	FCM						
μ MV operational cost	$C_{M,o}$	0.79	1.58	2.05	1.20	USD/mile	[67]–[69]				
μ MV cost	$C_{M,f}$	550	8,860	1,000	3,000	USD/ μ MV	[68]–[70]				
μ MV achievable speed	$v_{M,ij}$	15	10	15	15	mph	-				
μ MV life	t_M	0.085	7.0	10.0	10.0	year	[68]–[70]				
μ MV emissions	$m_{CO_2,M,tot}$	0.101	0.033	0.158	0.033	kg/mile	[68], [71]–[73]				
Time from \mathcal{G}_W to $\mathcal{G}_{R,M}$	t_{WM}	60	60	60	60	s	-				
Time from $\mathcal{G}_{R,M}$ to \mathcal{G}_W	t_{MW}	60	60	60	60	s	-				
Subway operational cost	$C_{S,o}$	100 %	150 %	200 %	148,000,000	222,000,000	295,000,000	14,500,000	USD/year	[74]	
Subway fixed cost	$C_{S,f}$	148,000,000	222,000,000	295,000,000	14,500,000	USD/train	[75]				
Train life	t_S	30	30	30	30	year	[75]				
Subway emissions per train	$m_{CO_2,S,tot}$	140,000	140,000	140,000	140,000	kg/year	[76]				
Train fleet baseline	$n_{S,base}$	112	112	112	112	train	[75]				
Subway service frequency	$\varphi_{j,baseline}$	1/6	1/6	1/6	1/6	1/min	-				
Time \mathcal{G}_W to \mathcal{G}_P	t_{WS}	60	60	60	60	s	-				

TABLE I: Parameters, variables, numbers, and units for the case studies.

	Mobility Type	Emissions	Cost	Speed	Reliability
Taxi	Point-to-point	High	High operational cost, medium fixed cost	High	Up to availability and congestion
AV	Point-to-point	High	Low operational cost, high fixed cost	High	Up to availability and congestion
μ MV	Point-to-point	Medium	Medium operational cost, low fixed cost	Low/Medium	Up to availability
Walking	Point-to-point	No emissions	Free	Low	High
Subway	Fixed hubs and routes	Low	Low	Medium	High

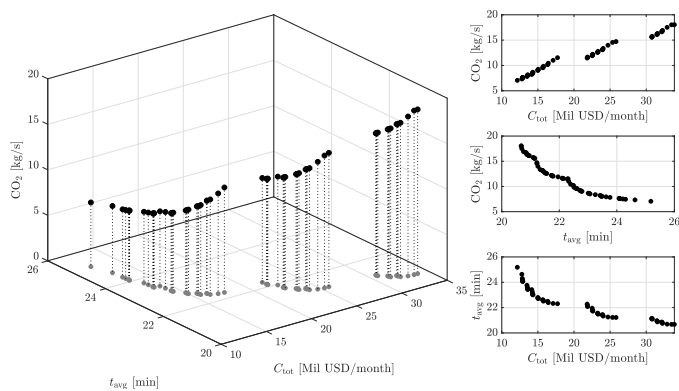
TABLE II: Comparison of the considered mobility solutions.

sion factor of 40 USD/kg [82]. Note that this transformation preserves the monotonicity of the CDPI and therefore integrates in our framework. The two-dimensional antichain and the corresponding central authority’s decisions are reported in Figure 4b. In general, as the municipality budget increases, the average travel time per trip required to satisfy the given demand decreases, reaching a minimum of about 20.7 min, with a monthly public expense of around 36 Mil USD/month. This configuration corresponds to a fleet of 4,000 AVs able to drive at 50 mph, and to the doubling of the current MetroRail train fleet. Furthermore, the smallest rational investment of 13 Mil USD/month leads to a 22 % higher average travel time, corresponding to the current situation, i.e., to a non-existent AVs fleet, and an unchanged subway infrastructure. Notably, an expense of 18 Mil USD/month (50 % lower than the highest rational investment) only increases the minimal required travel time by 8 %, requiring a fleet of 3,000 AVs able to drive at 45 mph and no acquisition of trains. Conversely, an expense of 15 Mil USD/month (just 2 Mil USD/month higher than the minimal rational investment) provides a 2 min shorter travel time. Finally, it is rational to improve the subway system starting from a budget of 23 Mil USD/month,

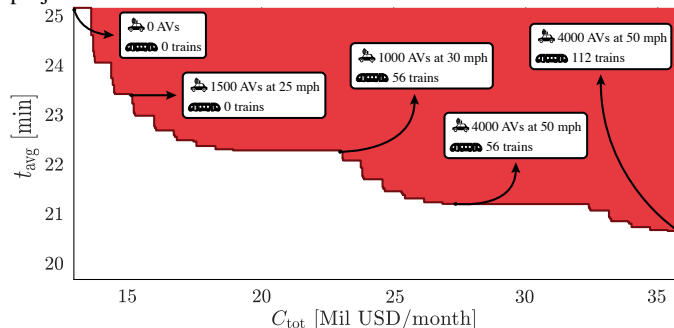
leading to a travel improvement of just 8 %. This trend can be explained with the high train acquisition cost and increased operation costs, related to the reinforcement of the subway system. This phenomenon is expected to be even more marked for other cities, considering the moderate operation costs of the MetroRail subway system, due to its automation and related benefits [83].

2) Speed-dependent automation costs:

2022: We report the results in Figure 5a. A comparison with our basic setting (cf. Figure 4) confirms the trends concerning public expense. Indeed, a public expense of 26 Mil USD/month (43 % lower than the highest rational expense) only increases the average travel time by 5 %, requiring a fleet of 2,000 AVs able to reach 30 mph and a subway reinforcement of 50 %. Nevertheless, our comparison shows two substantial differences. First, the budget required for an average travel time of 13 min is 25 % higher compared to S1. Second, the higher AV costs result in an average AVs fleet growth of 9 %, an average velocity reduction of 15 %, and an average train fleet growth of 14 %. The latter suggests a shift towards poorer AVs performance in favor of fleets reinforcements.



(a) Left: Three-dimensional representation of antichain elements and their projection in the cost-time space. Right: Two-dimensional projections.



(b) Results for constant automation costs. We report the two-dimensional representation of the antichain elements: The Pareto front is represented in dark red, and the upper set is the area above. We also report selected implementations corresponding to the highlighted antichain elements, in this case quantified in terms of achievable vehicle speed, AVs fleet size, and train fleet size³.

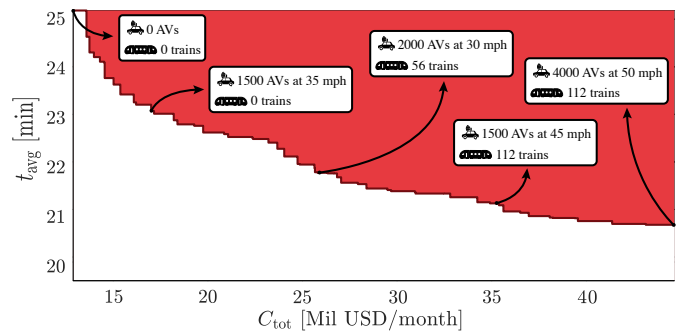
Fig. 4: Solution of the CDPI: Basic setting.

2025: The maximal rational budget is 23% lower than in the case of immediate deployment (Figure 5b). Further, the reduction in autonomy costs incentivizes the acquisition of more performant AVs, increasing the average vehicle speed by 14%. Hence, AVs and train fleets are 10% and 13% smaller.

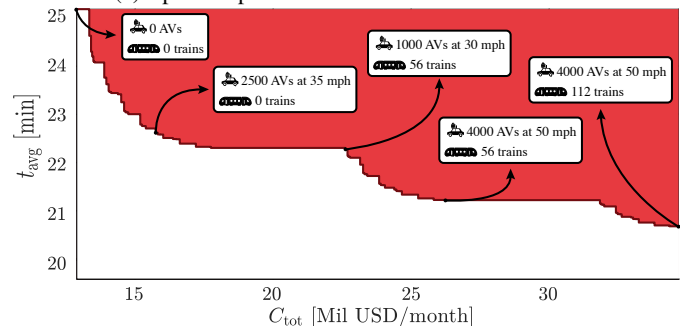
3) High automation costs analysis: Figure 6 shows the results for high automation costs. First, we observe a substantial shift towards larger train fleet sizes (65% larger than in S1) and smaller AVs fleets (55% smaller than in S1). Second, minimizing the average travel time entails an expense of approximately 68 Mil USD/month, basically doubling the investments observed in the basic setting.

4) MoD setting: We summarize the results for the MoD scenario in Figure 7. In particular, by comparing the MoD case with the 2025 setting, we can notice the game-changing properties that AVs introduce in the mobility ecosystem. In particular, the average train fleet size and the average vehicle fleet sizes increase by 130% and 66%, suggesting a clear transition in investments from public transit to AVs, and testifies to the interest in AMoD systems developed in the past years.

5) Impact of new transportation modes: To assess the impact of μM solutions, we compare the arising design solutions, reported in Figure 8, with their counterpart in S2 (cf. Figure 5).



(a) Speed-dependent automation costs in 2022.



(b) Speed-dependent automation costs in 2025.

Fig. 5: Results for the speed-dependent automation costs.

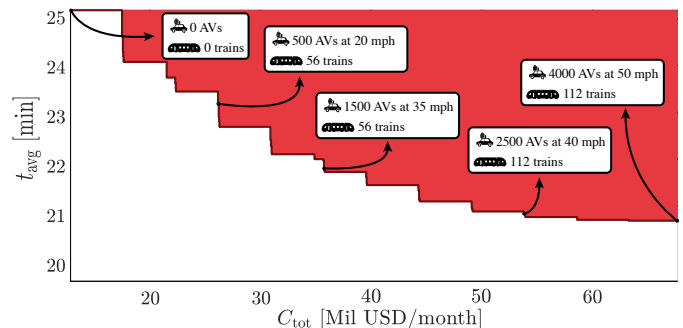


Fig. 6: Results for large automation costs.

2022: Figure 8a, together with Figure 5a, demonstrates an overall benefit from μM solutions. For instance, the most time-efficient solution in S2 yields an average travel time of 20.7 min at an expense of 45 Mil USD/month. The deployment of μM solutions lowers the average travel time achievable with the same expense by 10% (18.8 min) and allows for even lower average travel times, with a time-efficient solution of 17.6 min at an investment plan of 84 Mil USD/month. Overall, the average AVs fleet size and the average train fleet size are 35% and 6% smaller, in favor of an average μM fleet of 2,280 μMVs .

2025: Figure 8b, together with Figure 5b, shows that the benefit of μM solutions is less marked than in 2022. For instance, an expense of 35 Mil USD/month (same as the maximal expense in Figure 5b) results in an average travel time of 19.5 min, i.e., only 6% lower than in the case without μM . Furthermore, we observe an average AVs fleet size enlargement of 17%, and an average train fleet size

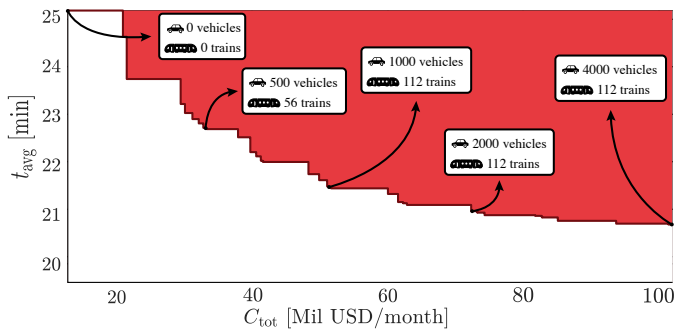


Fig. 7: Results for the MoD case.

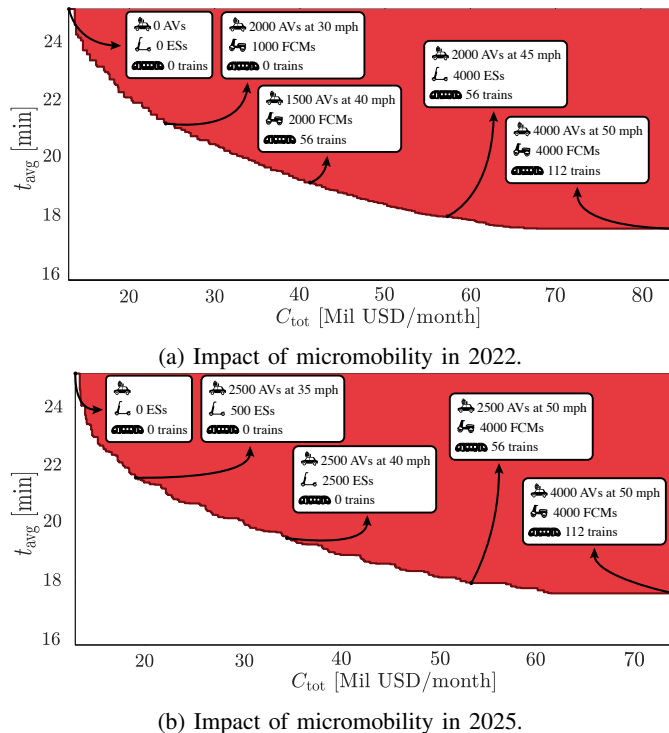


Fig. 8: Results for the impact of micromobility.

reduction of 27%. Finally, the comparison with the 2022 case highlights a μ MVs fleet reduction of 23%, which suggests the comparative advantage of AVs in the future. Indeed, the stronger the reduction of the cost of automation, the more investments in AVs are rational. The benefits of employing μ M solutions could therefore just be temporary, and gradually vanish as the costs of automation of AVs decrease.

6) *Pricing*: We report the results in Figure 9. In particular, we report the Pareto front between system performance and emissions (the two resources of the considered MDPI), as well as design choices for selected Pareto-optimal solutions, now including prices for AMoD and public transit services. We report three key observations. First, the most performing solution (which satisfies the cost-contributing constraint) features the usage of 4,000 AVs able to drive at 45 mph and an increment of 50% of the public transit fleets. The large usage of AVs is not only due to their efficiency, but also to the low price of 0.8 USD/mile. While this choice does not fully exploit the

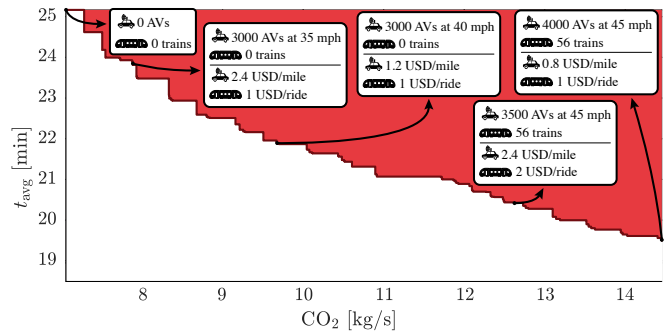


Fig. 9: Pricing and revenues case study. The Pareto front is in terms of system performance (average travel time) and produced externalities.

action space of the municipality (one could have larger fleets, more performant AVs, and more trains), it is the last one for which the weighted costs do not exceed the revenue. Second, we observe fewer solutions featuring an augmented train fleet, mainly because of the related onerous investments related (i.e., more AVs, not necessarily very performing, can bridge the system performance gap). Finally, comparing the emissions in Figure 9 and in Figure 4a suggests that bounding the allowed mobility system costs also prevents design options which are more pollutant from being chosen.

C. Discussion

First, the presented case studies showcase the ability of our framework to extract the set of rational design strategies for a future mobility system, including AVs, μ MVs, and public transit. This way, stakeholders such as mobility providers, transportation authorities, and policy makers can get transparent and interpretable insights on the impact of future interventions, inducing further reflection on this complex socio-technical problem. Note that this kind of results is only one of the many factors affecting negotiations when interacting with stakeholders. Second, we perform a sensitivity analysis through the variation of autonomy cost structures, and show the capacity of our framework to capture various models. On the one hand, this reveals a clear transition from small fleets of fast AVs (in the case of low autonomy costs) to large fleets of slow AVs (in the case of high autonomy costs). On the other hand, our studies highlight that investments in the subway infrastructure are rational only when large budgets are available. Indeed, the high train acquisition and operation costs lead to a comparative advantage of AV-based mobility. Finally, our case studies suggest that the deployment of μ M solutions is rational primarily on a short-term horizon: The lowering of automation costs could eventually make AVs the predominant actor in the future of urban mobility.

V. CONCLUSION

This paper leverages the mathematical theory of co-design to propose a co-design framework for future mobility systems. The nature of our framework offers a different viewpoint on the future mobility problem, enabling the modular and compositional interconnection of the design problems

of different mobility options and their optimization, given multiple objectives. Starting from the multi-commodity flow model of an intermodal mobility system, we designed AVs, μ MVs, and public transit both from a vehicle-centric and fleet-level perspective. Specifically, we studied the problem of deploying a fleet of self-driving vehicles providing on-demand mobility in cooperation with μ M solutions and public transit, adapting the speed achievable by AVs and μ MVs, their fleet sizes, and the service frequency of the subway lines. Our framework allows stakeholders involved in the mobility ecosystem, from vehicle developers all the way to mobility-as-a-service companies and central authorities, to characterize rational trajectories for technology and investment development. We showcased both the developer and the user views of the framework, explaining how practitioners can easily use their models within it. The proposed methodology is showcased in a case study based on data for Washington D.C., USA. Notably, we highlighted how our problem formulation allows for a systematic analysis of incomparable objectives, such as public expense, average travel time, and emissions, providing stakeholders with analytical insights for the socio-technical design of future mobility systems. This work urges the following future research streams:

Modeling: First, we would like to capture heterogeneous fleets of AVs, with different autonomy pipelines, propulsion systems, and passenger capacity. For instance, the modular nature of the framework allows one to easily include complex autonomy models in the design problem of the AV fleet [7], [8]. Second, we would like to investigate variable demand models. Third, we would like to analyze the interactions between multiple stakeholders in the mobility ecosystem, characterized by conflicting interests and different action spaces. It is advantageous to formulate this as a game, and to characterize potentially arising equilibria [84], [85], possibly leveraging recent results in posetal games [86]. This might bring realism and effectiveness in the actionable information proposed to the mobility stakeholders. Finally, we would like to explicitly include (and not just via costs) more elements of urban design in the co-design model, to account for more realistic scenarios [87]. These include parking spaces and autonomy-enabling infrastructure.

Algorithms: We are interested in tailoring general co-design algorithmic frameworks to the particular case of transportation design problems, leveraging their specific structure, and characterizing their solutions. In particular, we would like to study adaptive approaches to cleverly simulate mobility systems.

APPENDIX

A. Nomenclature

AMoD-related symbols

s_{ij}	Length of arc $\langle i, j \rangle$
c	Edge-coloring maps
\mathcal{A}	Set of arcs of a digraph
\mathcal{G}	Digraph
\mathcal{V}	Set of vertices of a digraph
ρ	Revenue
q	Travel demand

s_{cycle}	Length of cycle
v_V	Speed AV
χ	Fraction of the revenue to cover costs
v_M	Speed μ M
β	Threshold for minimal speed
α	Demand rate
α_{tot}	Total demand rate
γ	Energy consumption to CO ₂ emissions
$C_{V,f}$	Vehicle fix cost
$m_{\text{CO}_2,M,\text{tot}}$	Emissions μ MV
$m_{\text{CO}_2,S,\text{tot}}$	Emissions subway
$m_{\text{CO}_2,V,\text{tot}}$	Emissions AV
φ_j	Subway service frequency
$\varphi_{j,\text{base}}$	Subway baseline service frequency
l_M	Lifetime μ MV
l_S	Lifetime subway train
l_V	Lifetime AV
red	Graph reduction maps
$n_{M,\text{max}}$	Fleet size μ MVs
n_S	Fleet size subway
$n_{M,u}$	Used μ MVs
$n_{V,u}$	Used AVs
$n_{V,\text{max}}$	Fleet size AVs
π	Projection maps
\mathbf{G}	Set of graphs
$C_{M,f}$	μ MV fix cost
$C_{S,f}$	Subway fix cost
$C_{M,o}$	μ MV operational cost
$C_{S,o}$	Subway operational cost
$C_{V,o}$	AV operational cost
C_{tot}	Total cost
$s_{M,\text{tot}}$	Total distance μ MV
$s_{V,\text{tot}}$	Total distance AV
t_{ij}	Travel time of arc $\langle i, j \rangle$
t_{avg}	Average travel time
$f_m(i, j)$	Flow of customers per unit time on arc $\langle i, j \rangle$
$f_{0,V}(i, j)$	Flow of empty AVs on arc $\langle i, j \rangle$
$f_{0,M}(i, j)$	Flow of empty μ MVs on arc $\langle i, j \rangle$
$f_{\text{tot},M}(i, j)$	Total flow of μ MVs on arc $\langle i, j \rangle$
$f_{\text{tot},V}(i, j)$	Total flow of AVs on arc $\langle i, j \rangle$
v_W	Walking speed
u_{ij}	Baseline usage for arc $\langle i, j \rangle$
e_{ij}	Energy consumption for arc $\langle i, j \rangle$
k_{ij}	Normal capacity of arc $\langle i, j \rangle$
$v_{L,ij}$	Speed limit for arc $\langle i, j \rangle$
$v_{M,ij}$	Speed of μ MVs on arc $\langle i, j \rangle$
$v_{V,ij}$	Speed of AVs on arc $\langle i, j \rangle$

Co-design-related symbols

\perp, \top	Bottom and top of a poset
\mathcal{P}	Poset and powerset
\mathcal{F}	Functionalities
\mathcal{R}	Resources
d	Design problem
\mathcal{AP}	Set of antichains for poset \mathcal{P}
prov	Implementation-to-functionality map
reqs	Implementation-to-resources map

B. Background on solution of co-design problems

For the convenience of the reader, in the following we report technical results from [3], [6].

1) *Solution of CDPI*: We first recall concepts related to fixed points.

Definition A.1 (Least fixed point). A *least fixed point* of $f: \mathcal{P} \rightarrow \mathcal{P}$ is the minimum (if it exists) of the set of fixed points of f :

$$\text{lfp}(f) = \min_{\leq_{\mathcal{P}}} \{x \in \mathcal{P} : f(x) = x\}.$$

A least fixed point might not exist. Monotonicity of the map f and completeness of the partial orders is sufficient to ensure existence.

Definition A.2 (Completeness). A poset is a *directed complete partial order (DCPO)* if each of its directed subsets has a supremum (least of upper bounds). It is a *complete partial order (CPO)* if it also has a bottom.

Example A.3. Consider $\mathbb{R}_{\geq 0} = \{x \in \mathbb{R} \mid x \geq 0\}$, which has a bottom $\perp = 0$. One can make $\langle \mathbb{R}_{\geq 0}, \leq \rangle$ a CPO by adding an artificial top element \top , by defining $\overline{\mathbb{R}_{\geq 0}} := \mathbb{R}_{\geq 0} \cup \{\top\}$, and extending the partial order \leq such that $a \leq \top$ for all $a \in \mathbb{R}_{\geq 0}$.

Lemma A.4 (Lemma 3 in [3]). *If \mathcal{P} is a CPO and $f: \mathcal{P} \rightarrow \mathcal{P}$ is monotone, then $\text{lfp}(f)$ exists.*

Assuming Scott continuity of f , Kleene's algorithm is a systematic procedure to find the least fixed point.

Definition A.5 (Scott continuity). A map $f: \mathcal{P} \rightarrow \mathcal{Q}$ between DCPOs is *Scott continuous* if and only if, for each directed subset $D \subseteq \mathcal{P}$, the image $f(D)$ is directed, and $f(\sup D) = \sup f(D)$.

Lemma A.6 (Lemma 4 in [3]). *Assume \mathcal{P} is a CPO and $f: \mathcal{P} \rightarrow \mathcal{P}$ is Scott continuous. Then, the least fixed point of f is the supremum of the Kleene ascent chain*

$$\perp \preceq f(\perp) \preceq f(f(\perp)) \preceq \dots \preceq f^{(n)}(\perp) \preceq \dots$$

Note that a sufficient condition is to assume all posets to be finite.

Theorem A.7. *The map h for a CDPI has an explicit expression in terms of the maps h_a of its subproblems.*

We report the specific definition of these maps.

Definition A.8 (Series). For two maps $h_1: \mathcal{F}_1 \rightarrow \mathcal{AR}_1$, $h_2: \mathcal{F}_2 \rightarrow \mathcal{AR}_2$, if $\mathcal{R}_1 = \mathcal{F}_2$, define

$$h_1 \circledast h_2: \mathcal{F}_1 \rightarrow \mathcal{AR}_2$$

$$f_1 \mapsto \text{Min}_{\leq_{\mathcal{R}_2}} \bigcup_{s \in h_1(f)} h_2(s).$$

Definition A.9 (Parallel). For two maps $h_1: \mathcal{F}_1 \rightarrow \mathcal{AR}_1$, $h_2: \mathcal{F}_2 \rightarrow \mathcal{AR}_2$, define

$$h_1 \otimes h_2: \mathcal{F}_1 \times \mathcal{F}_2 \rightarrow \mathcal{A}(\mathcal{R}_1 \times \mathcal{R}_2)$$

$$\langle f_1, f_2 \rangle \mapsto h_1(f_1) \times h_2(f_2).$$

Definition A.10 (Loop). For $h: \mathcal{F} \times \mathcal{R} \rightarrow \mathcal{AR}$ define

$$h^\dagger: \mathcal{F} \rightarrow \mathcal{AR}$$

$$f \mapsto \text{lfp}(\Psi_f^h),$$

where

$$\Psi_f^h: \mathcal{AR} \rightarrow \mathcal{AR}$$

$$R \mapsto \text{Min}_{\leq_{\mathcal{R}}} \bigcup_{r \in R} h(f, r) \cap \uparrow \{r\},$$

where \uparrow represents the upper closure operator.

Definition A.11 (Coproduct). For $h_1, h_2: \mathcal{F} \rightarrow \mathcal{AR}$, define

$$h_1 \vee h_2: \mathcal{F} \rightarrow \mathcal{AR}$$

$$f \mapsto \text{Min}_{\leq_{\mathcal{R}}} (h_1(f) \cup h_2(f)).$$

Algorithm sketch: Given the aforementioned discoveries, the algorithmic procedure to solve co-design problems is the following. 1) Take an arbitrary CDPI (inrerconnection of MDPIs). 2) Flatten it to a graph. 3) Re-write the graph in form of a series of series-parallel and feedback graphs. 4) Write the graph as a tree of composition operations. 5) Run Kleene's iteration recursively on the graph.

2) *Complexity of the solution:* The results for complexity are described in [3]. Consider a CDPI. The space of the solution is bounded by the width of \mathcal{R} . At each iteration, the number of evaluations of each component is linear in the number of options. The number of execution steps depends on the height of the poset of antichains of \mathcal{R} .

C. Proofs

Proof of Lemma III.2. Consider partial orders A, B, C and maps $f, g, h: A \rightarrow B$. Clearly $f \preceq_{B^A} g$. Furthermore, if $f \preceq_{B^A} g$ and $g \preceq_{C^B} h$ (i.e., $f(a) \preceq_B g(a)$ and $g(a) \preceq h(a)$, $\forall a \in A$), then $f(a) \preceq_B h(a)$ $\forall a \in A$, implying $f \preceq_{B^A} h$. Finally, if $f \preceq_{B^A} g$ and $g \preceq_{B^A} f$, one has $f = g$. \square

Proof of Lemma III.4. Consider $\mathcal{G}_1, \mathcal{G}_2, \mathcal{G}_3 \in \mathbf{G}$ with $\mathcal{G}_1 = \langle \mathcal{V}_1, \mathcal{A}_1, c_1 \rangle$, $\mathcal{G}_2 = \langle \mathcal{V}_2, \mathcal{A}_2, c_2 \rangle$, $\mathcal{G}_3 = \langle \mathcal{V}_3, \mathcal{A}_3, c_3 \rangle$, and $c_i: \mathcal{A}_i \rightarrow C$. Clearly $\mathcal{G}_1 \preceq_{\mathbf{G}} \mathcal{G}_1$, since $\mathcal{V}_1 \subseteq \mathcal{V}_1$, $\mathcal{A}_1 \subseteq \mathcal{A}_1$, and $c_1 \succeq_{C^{\mathcal{A}_1}} c_1$. Furthermore, given $\mathcal{G}_1 \preceq_{\mathbf{G}} \mathcal{G}_2$ and $\mathcal{G}_2 \preceq_{\mathbf{G}} \mathcal{G}_3$ (i.e., $\mathcal{V}_1 \subseteq \mathcal{V}_2 \subseteq \mathcal{V}_3$, $\mathcal{A}_1 \subseteq \mathcal{A}_2 \subseteq \mathcal{A}_3$, $c_1 \succeq_{C^{\mathcal{A}_1}} c_2|_{\mathcal{A}_1}$, and $c_2 \succeq_{C^{\mathcal{A}_2}} c_3|_{\mathcal{A}_2}$), one has $\mathcal{V}_1 \subseteq \mathcal{V}_3$, $\mathcal{A}_1 \subseteq \mathcal{A}_3$, and $c_1 \succeq_{C^{\mathcal{A}_1}} c_3|_{\mathcal{A}_1}$, implying $\mathcal{G}_1 \preceq_{\mathbf{G}} \mathcal{G}_3$. Finally, it is easy to see that $\mathcal{G}_1 \preceq_{\mathbf{G}} \mathcal{G}_2$ and $\mathcal{G}_2 \preceq_{\mathbf{G}} \mathcal{G}_1$ implies $\mathcal{G}_1 = \mathcal{G}_2$. \square

Proof of Lemma III.7. Consider $Q_1, Q_2, Q_3 \in \mathcal{Q}$. Clearly $Q_1 \preceq_{\mathcal{Q}} Q_1$. Let $Q_1 \preceq_{\mathcal{Q}} Q_2$ and $Q_2 \preceq_{\mathcal{Q}} Q_3$, and let $\langle o^1, d^1, \alpha^1 \rangle \in Q_1$. Since $Q_1 \preceq_{\mathcal{Q}} Q_2$, there is $\langle o^2, d^2, \alpha^2 \rangle \in Q_2$ such that $o^1 = o^2$, $d^1 = d^2$, and $\alpha^2 \geq \alpha^1$. Since $Q_2 \preceq_{\mathcal{Q}} Q_3$, there is $\langle o^3, d^3, \alpha^3 \rangle \in Q_3$ such that $o^2 = o^3$, $d^2 = d^3$, and $\alpha^3 \geq \alpha^2$. So, $o^1 = o^3$, $d^1 = d^3$, $\alpha^3 \geq \alpha^1$, proving that $Q_1 \preceq_{\mathcal{Q}} Q_3$. Finally, $Q_1 \preceq_{\mathcal{Q}} Q_2$ and $Q_2 \preceq_{\mathcal{Q}} Q_1$ implies $Q_1 = Q_2$ (given that origin-destination pairs are not repeated). \square

Proof of Lemma III.8. We need to prove that for $v_1, v_2 \in \mathbb{R}_{\geq 0}$ one has: $v_1 \leq v_2 \Rightarrow \text{red}_{\mathbb{R}, \mathcal{V}}(v_1) \preceq_{\mathbf{G}} \text{red}_{\mathbb{R}, \mathcal{V}}(v_2)$. Following the definition, $\text{red}_{\mathbb{R}, \mathcal{V}}(v_1)$ and $\text{red}_{\mathbb{R}, \mathcal{V}}(v_2)$ will share the same set of vertices (satisfying the vertex condition). Furthermore, $v_1 \leq v_2$ implies that the arcs \mathcal{A}_1 of $\text{red}_{\mathbb{R}, \mathcal{V}}(v_1)$ will be a subset of the set of arcs \mathcal{A}_2 of $\text{red}_{\mathbb{R}, \mathcal{V}}(v_2)$. Finally, the edge colors remain unchanged, except for speed-related one. Let c_1, c_2 the colors associated to $\text{red}_{\mathbb{R}, \mathcal{V}}(v_1)$ and $\text{red}_{\mathbb{R}, \mathcal{V}}(v_2)$, respectively. Clearly $\min\{v_1, x\} \leq \min\{v_2, x\}$ for any $x \in$

$\mathbb{R}_{\geq 0}$. This, together with Equation (4), gives $c_1 \succeq_{\mathcal{C}^{\mathcal{A}_1}} c_2$, proving monotonicity. \square

Proof of Lemma III.9. $C_{V,f}, C_{V,o}$ are monotone functions of the AV's achievable speed. Leveraging Lemma III.8, we know that the serviced network is a monotone function of the speed. \square

Proof of Lemma III.10. We need to prove that given $v_1, v_2 \in \mathbb{R}_{\geq 0}$, one has: $v_1 \leq v_2 \Rightarrow \text{red}_{R,M}(v_1) \preceq_{\mathbf{G}} \text{red}_{R,M}(v_2)$. First, notice that sets of vertices and arcs are preserved by $\text{red}_{R,M}$. Second, the argument for the edge attributes is analogous to the one in the proof of Lemma III.8. The two facts together prove monotonicity. \square

Proof of Lemma III.11. $C_{M,f}, C_{M,o}$ are monotone functions of the μ MV's achievable speed. Leveraging Lemma III.10, we know that the serviced network is a monotone function of the speed. \square

Proof of Lemma III.12. We need to prove that given $n_1, n_2 \in \mathbb{R}_{\geq 0}$, one has: $n_1 \leq n_2 \Rightarrow \text{red}_P(n_1) \preceq_{\mathbf{G}} \text{red}_P(n_2)$. Again, we notice that the set of vertices and arcs are preserved by red_P . Furthermore, $n_1 \leq n_2$ implies that $t_{WS} + \frac{n_{S,\text{base}}}{2n_1\varphi_{j,\text{base}}} \geq t_{WS} + \frac{n_{S,\text{base}}}{2n_2\varphi_{j,\text{base}}}$, proving monotonicity. \square

Proof of Lemma III.13. First, notice that C_S and $m_{\text{CO}_2,S,\text{tot}}$ are monotone functions of n_S . Furthermore, leveraging Lemma III.12, we know that the serviced network relates monotonically to n_S . \square

Proof of Lemma III.14. Let $r \preceq_{\mathbf{G}^2 \times \mathbb{N} \times \mathbb{R}_{\geq 0}^3} r'$. Since all feasible solutions of (8) with r remain feasible with r' , $\bar{d}_{\text{IAMOD}}(q^*, r) \subseteq \bar{d}_{\text{IAMOD}}(q^*, r')$ for all $q \in \mathcal{Q}$. Similarly, let $q' \preceq_{\mathcal{Q}} q$. Since all feasible solutions of (8) remain feasible (possibly by replacing demand with empty vehicles and by artificially adding loops to the graph), $\bar{d}_{\text{IAMOD}}(q', r) \subseteq \bar{d}_{\text{IAMOD}}(q, r)$ for all $r \in \mathbf{G}^2 \times \mathbb{N} \times \mathbb{R}_{\geq 0}^3$. This proves monotonicity. \square

Proof of Lemmas III.15 and III.16. The proofs parallel the proof of Lemma III.14. \square

Proof of Lemmas III.17, III.18, and III.19. The MDPIs are monotone, since they consist of the valid composition of monotone MDPIs [3]. \square

REFERENCES

- [1] G. Zardini, N. Lanzetti, M. Pavone, and E. Frazzoli, "Analysis and control of autonomous mobility-on-demand systems," *Annual Review of Control, Robotics, and Autonomous Systems*, vol. 5, no. 1, 2022.
- [2] T. Yigitcanlar, M. Wilson, and M. Kamruzzaman, "Disruptive impacts of automated driving systems on the built environment and land use: An urban planner's perspective," *Journal of Open Innovation: Technology, Market, and Complexity*, vol. 5, no. 2, p. 24, 2019.
- [3] A. Censi, "A mathematical theory of co-design," *arXiv preprint arXiv:1512.08055v7*, 2015.
- [4] —, "A class of co-design problems with cyclic constraints and their solution," *IEEE Robotics and Automation Letters*, vol. 2, pp. 96–103, 2017.
- [5] —, "Uncertainty in monotone co-design problems," *IEEE Robotics and Automation Letters*, vol. 2, no. 3, pp. 1556–1563, 2017.
- [6] A. Censi, J. Lorand, and G. Zardini, *Applied Compositional Thinking for Engineers*, 2022, work in progress book. [Online]. Available: <https://bit.ly/3H6pwMo>
- [7] G. Zardini, D. Milojevic, A. Censi, and E. Frazzoli, "Co-design of embodied intelligence: A structured approach," in *2021 IEEE/RSJ International Conference on Intelligent Robots and Systems (IROS)*, 2021, pp. 7536–7543.
- [8] G. Zardini, A. Censi, and E. Frazzoli, "Co-design of autonomous systems: From hardware selection to control synthesis," in *2021 European Control Conference (ECC)*, 2021, pp. 682–689.
- [9] M. Salazar, N. Lanzetti, F. Rossi, M. Schiffer, and M. Pavone, "Intermodal autonomous mobility-on-demand," *IEEE Transactions on Intelligent Transportation Systems*, vol. 21, no. 9, pp. 3946–3960, 2020.
- [10] R. Z. Farahani, E. Miandoabchi, W. Y. Szeto, and H. Rashidi, "A review of urban transportation network design problems," *European Journal of Operational Research*, vol. 229, pp. 281–302, 2013.
- [11] V. Guihaire and J.-K. Hao, "Transit network design and scheduling: A global review," *Transportation Research Part B: Methodological*, vol. 42, pp. 1251–1273, 2008.
- [12] A. Loder, M. C. Bliemer, and K. W. Axhausen, "Optimal pricing and investment in a multi-modal city — introducing a macroscopic network design problem based on the mfd," *Transportation Research Part A: Policy and Practice*, vol. 156, pp. 113–132, 2022.
- [13] Z. Cong, B. De Schutter, and R. Babuska, "Co-design of traffic network topology and control measures," *Transportation Research Part C: Emerging Technologies*, vol. 54, pp. 56–73, 2015.
- [14] Q. Luo, S. Li, and R. C. Hampshire, "Optimal design of intermodal mobility networks under uncertainty: Connecting micromobility with mobility-on-demand transit," *EURO Journal on Transportation and Logistics*, vol. 10, p. 100045, 2021. [Online]. Available: <https://www.sciencedirect.com/science/article/pii/S2192437621000170>
- [15] R. O. Arbex and C. B. da Cunha, "Efficient transit network design and frequencies setting multi-objective optimization by alternating objective genetic algorithm," *Transportation Research Part B: Methodological*, vol. 81, pp. 355–376, 2015.
- [16] L. Sun, J. G. Jin, D.-H. Lee, K. W. Axhausen, and A. Erath, "Demand-driven timetable design for metro services," *Transportation Research Part C: Emerging Technologies*, vol. 46, pp. 284–299, 2014.
- [17] S. Su, X. Li, T. Tang, and Z. Gao, "A subway train timetable optimization approach based on energy-efficient operation strategy," *IEEE Transactions on Intelligent Transportation Systems*, vol. 14, no. 2, pp. 883–893, 2013.
- [18] J. A. Barrios and J. D. Godier, "Fleet sizing for flexible carsharing systems: Simulation-based approach," *Transportation Research Record: Journal of the Transportation Research Board*, vol. 2416, pp. 1–9, 2014.
- [19] D. J. Fagnant and K. M. Kockelman, "Dynamic ride-sharing and fleet sizing for a system of shared autonomous vehicles in austin, texas," *Transportation*, vol. 45, no. 1, pp. 143–158, 2018.
- [20] M. M. Vazifeh, P. Santi, G. Resta, S. H. Strogatz, and C. Ratti, "Addressing the minimum fleet problem in on-demand urban mobility," *Nature*, vol. 557, no. 7706, p. 534, 2018.
- [21] P. M. Boesch, F. Ciari, and K. W. Axhausen, "Autonomous vehicle fleet sizes required to serve different levels of demand," *Transportation Research Record: Journal of the Transportation Research Board*, vol. 2542, no. 1, pp. 111–119, 2016.
- [22] M. Meghjani, S. D. Pendleton, K. A. Marczuk, Y. H. Eng, X. Shen, M. H. Ang, and D. Rus, "Multi-class fleet sizing and mobility on demand service," in *International Conference on Complex Systems Design & Management*. Springer, 2018, pp. 37–49.
- [23] J. Narayan, O. Cats, N. van Oort, and S. P. Hoogendoorn, "Fleet size determination for a mixed private and pooled on-demand system with elastic demand," *Transportmetrica A: Transport Science*, vol. 17, no. 4, pp. 897–920, 2021.
- [24] K. Spieser, K. Treleven, R. Zhang, E. Frazzoli, D. Morton, and M. Pavone, "Toward a systematic approach to the design and evaluation of automated mobility-on-demand systems: A case study in singapore," in *Road vehicle automation*. Springer, 2014, pp. 229–245.
- [25] H. Zhang, C. J. Sheppard, T. E. Lipman, and S. J. Moura, "Joint fleet sizing and charging system planning for autonomous electric vehicles," *IEEE Transactions on Intelligent Transportation Systems*, vol. 21, no. 11, pp. 4725–4738, 2019.
- [26] G. J. Beaujon and M. A. Turnquist, "A model for fleet sizing and vehicle allocation," *Transportation Science*, vol. 25, no. 1, pp. 19–45, 1991.
- [27] A. Wallar, W. Schwarting, J. Alonso-Mora, and D. Rus, "Optimizing multi-class fleet compositions for shared mobility-as-a-service," in *Proc. IEEE Int. Conf. on Intelligent Transportation Systems*. IEEE, 2019, pp. 2998–3005.
- [28] H. K. Pinto, M. F. Hyland, H. S. Mahmassani, and I. Ö. Verbas, "Joint design of multimodal transit networks and shared autonomous mobility fleets," *Transportation Research Part C: Emerging Technologies*, vol. 113, pp. 2–20, 2020.

- [29] T. Seo and Y. Asakura, "Multi-objective linear optimization problem for strategic planning of shared autonomous vehicle operation and infrastructure design," *IEEE Transactions on Intelligent Transportation Systems*, vol. 23, no. 4, pp. 3816–3828, 2021.
- [30] S. Shaheen and A. Cohen, "Shared micromobility policy toolkit: Docked and dockless bike and scooter sharing," 2019.
- [31] M. Ghamami and M. Shojaei, "Introducing a design framework for a multi-modal public transportation system, focusing on mixed-fleet bike-sharing systems," *Transportation Research Record: Journal of the Transportation Research Board*, vol. 2672, no. 36, pp. 103–115, 2018.
- [32] C.-C. Lu, "Robust multi-period fleet allocation models for bike-sharing systems," *Networks and Spatial Economics*, vol. 16, no. 1, pp. 61–82, 2016.
- [33] S. Yan, C.-C. Lu, and M.-H. Wang, "Stochastic fleet deployment models for public bicycle rental systems," *International Journal of Sustainable Transportation*, vol. 12, no. 1, pp. 39–52, 2018.
- [34] Q. Luo, S. Li, and R. C. Hampshire, "Optimal design of intermodal mobility networks under uncertainty: Connecting micromobility with mobility-on-demand transit," *EURO Journal on Transportation and Logistics*, p. 100045, 2021.
- [35] J. Y. Chow and H. R. Sayarshad, "Symbiotic network design strategies in the presence of coexisting transportation networks," *Transportation Research Part B: Methodological*, vol. 62, pp. 13–34, 2014.
- [36] D. Kondor, X. Zhang, M. Meghiani, P. Santi, J. Zhao, and C. Ratti, "Estimating the potential for shared autonomous scooters," *IEEE Transactions on Intelligent Transportation Systems*, pp. 1–12, 2021.
- [37] S.-Y. Lu, W. ElMaraghy, G. Schuh, and R. Wilhelm, "A scientific foundation of collaborative engineering," *CIRP annals*, vol. 56, no. 2, pp. 605–634, 2007.
- [38] W. Zhang and J. Yin, "Exploring semantic web technologies for ontology-based modeling in collaborative engineering design," *The International Journal of Advanced Manufacturing Technology*, vol. 36, no. 9, pp. 833–843, 2008.
- [39] G. Zardini, N. Lanzetti, M. Salazar, A. Censi, E. Frazzoli, and M. Pavone, "On the co-design of av-enabled mobility systems," in *2020 IEEE 23rd International Conference on Intelligent Transportation Systems (ITSC)*, 2020, pp. 1–8.
- [40] —, "Towards a co-design framework for future mobility systems," in *Annual Meeting of the Transportation Research Board*, Washington D.C., United States, Jan. 2020.
- [41] B. A. Davey and H. A. Priestley, *Introduction to Lattices and Order*, second edition ed. Cambridge University Press, 2002.
- [42] B. Fong and D. I. Spivak, *An invitation to applied category theory: seven sketches in compositionality*. Cambridge University Press, 2019.
- [43] P. Blackwell, K. Carter-Cram, E. Pape, and S. Islam, "E-scooter impact on traffic congestion," 2019.
- [44] C. F. Daganzo and N. Geroliminis, "An analytical approximation for the macroscopic fundamental diagram of urban traffic," *Transportation Research Part B: Methodological*, vol. 42, no. 9, pp. 771–781, 2008.
- [45] A. Henao and W. E. Marshall, "The impact of ride-hailing on vehicle miles traveled," *Transportation*, vol. 46, no. 6, pp. 2173–2194, 2019.
- [46] D. Dahl. (2018) If you're annoyed at drivers going under the speed limit, the problem isn't them, it's you. The Bellingham Herald. The Bellingham Herald. Available online.
- [47] A. Mas-Colell, M. D. Whinston, and J. R. Green, *Microeconomic Theory*. Oxford Univ. Press, 1995.
- [48] D. C. Richards, "Relationship between speed and risk of fatal injury: Pedestrians and car occupants," Department for Transport: London, Tech. Rep., 2010.
- [49] A. Horni, K. Nagel, and K. W. Axhausen, Eds., *The Multi-Agent Transport Simulation MATSim*. Ubiquity Press, 2016.
- [50] N. H. Gartner, "Optimal traffic assignment with elastic demands: A review part i. analysis framework," *Transportation Science*, vol. 14, no. 2, pp. 174–191, 1980.
- [51] —, "Optimal traffic assignment with elastic demands: a review part ii. algorithmic approaches," *Transportation Science*, vol. 14, no. 2, pp. 192–208, 1980.
- [52] M. Haklay and P. Weber, "OpenStreetMap: User-generated street maps," *IEEE Pervasive Computing*, vol. 7, no. 4, pp. 12–18, 2008.
- [53] GTFS. (2019) GTFS: Making public transit data universally accessible. Available online at <https://gtfs.org/>.
- [54] ODDC. (2017) Taxicab trips in 2016. Open Data DC. Open Data DC. Available online at <https://opendata.dc.gov/search?q=taxicabs>.
- [55] PIM. (2012) Metrorail ridership by origin and destination. Plan It Metro. Plan It Metro. Available online at <https://planitmetro.com/2012/10/31/data-download-metrorail-ridership-by-origin-and-destination/>.
- [56] F. Siddiqui. (2018) As ride hailing booms in d.c., it's not just eating in the taxi market – it's increasing vehicle trips. The Washington Post. available online.
- [57] DoA, Ed., *Military Police Traffic Operations*. Department of the Army, 1977.
- [58] S. Dixon, H. Irshad, and V. White, "Deloitte city mobility index – washington d.c." Deloitte, Tech. Rep., 2018.
- [59] N. Pavlenko, P. Slowik, and N. Lutsey, "When does electrifying shared mobility make economic sense?" The International Council on Clean Transportation, Tech. Rep., 2019.
- [60] A. Censi. (2019) Monotone co-design problems. Available online: <https://co-design.science/index.html>.
- [61] P. M. Boesch, F. Becker, H. Becker, and K. W. Axhausen, "Cost-based analysis of autonomous mobility services," *Transport Policy*, vol. 64, pp. 76–91, 2018.
- [62] D. J. Fagnant and K. Kockelman, "Preparing a nation for autonomous vehicles: opportunities, barriers and policy recommendations," *Transportation Research Part A: Policy and Practice*, vol. 77, pp. 167–181, 2015.
- [63] G. S. Bauer, J. B. Greenblatt, and B. F. Gerke, "Cost, energy, and environmental impact of automated electric taxi fleets in manhattan," *Environmental Science & Technology*, vol. 52, no. 8, pp. 4920–4928, 2018.
- [64] T. Litman, "Autonomous vehicle implementation predictions – implications for transport planning," Victoria Transport Policy Institute, Tech. Rep., 2019.
- [65] Z. Wadud, "Fully automated vehicles: A cost of ownership analysis to inform early adoption," *Transportation Research Part A: Policy and Practice*, vol. 101, pp. 163–176, 2017.
- [66] W. Time. (2018, Mar.) Carbon footprint data. Wired. Available at <https://api.wattime.org>.
- [67] D. Schellong, P. Sadek, C. Schaezberger, and T. Barrack, "The promise and pitfalls of e-scooter sharing," Boston Consulting Group, Tech. Rep., 2019.
- [68] D. C.-H. Chao, P. J. Van Duijsen, J. Hwang, and C.-W. Liao, "Modeling of a taiwan fuel cell powered scooter," in *2009 International Conference on Power Electronics and Drive Systems (PEDS)*. IEEE, 2009, pp. 913–919.
- [69] G. of the District of Columbia, "District of columbia, capitel bikeshare development plan," District of Columbia, Tech. Rep., 2015.
- [70] S. Korus. (2019) Electric scooters: The unit economics may spell trouble. ARK Invest Research Industrial. ARK Invest. Available online.
- [71] J. Hollingsworth, B. Copeland, and J. X. Johnson, "Are e-scooters polluters? the environmental impacts of shared dockless electric scooters," *Environmental Research Letters*, vol. 14, no. 8, p. 084031, 2019.
- [72] Z. Kou, X. Wang, S. F. A. Chiu, and H. Cai, "Quantifying greenhouse gas emissions reduction from bike share systems: a model considering real-world trips and transportation mode choice patterns," *Resources, Conservation and Recycling*, vol. 153, p. 104534, 2020.
- [73] P. Van Zyl, P. van Mensch, N. Ligterink, R. Droegge, and G. Kadijk, "Update emission model for two wheeled mopeds," *TNO report, TNO*, p. R11088, 2014.
- [74] WMATA, "Fy2018 proposed budget," Washington Metropolitan Area Transit Authority, Tech. Rep., 2017.
- [75] L. Aratani. (2015) Metro to debut first of its 7000-series cars on blue line on april 14. The Washington Post. available online.
- [76] WMATA, "Sustainability report 2018," Washington Metropolitan Area Transit Authority, Tech. Rep., 2018.
- [77] H. Becker, F. Becker, R. Abe, S. Bekhor, P. F. Belgiawan, J. Compostella, E. Frazzoli, L. M. Fulton, D. G. Bicudo, K. M. Gurumurthy, et al., "Impact of vehicle automation and electric propulsion on production costs for mobility services worldwide," *Transportation Research Part A: Policy and Practice*, vol. 138, pp. 105–126, 2020.
- [78] J. H. Gawron, G. A. Keoleian, R. D. De Kleine, T. J. Wallington, and K. Hyung Chul, "Life cycle assessment of connected and automated vehicles: Sensing and computing subsystem and vehicle level effects," *Environmental Science & Technology*, vol. 52, pp. 3249–3256, 2018.
- [79] WCP, "The automotive lidar market," Woodside Capital Partners, Tech. Rep., 2018.
- [80] P. Lienert. (2019) Cost of driverless vehicles to drop dramatically: Delphi ceo. Insurance Journal. available online.
- [81] K. Korosec. (2019) Uber spent usd 457 million on self-driving and flying car r&d last year. TechCrunch. TechCrunch. Available online.
- [82] P. Howard and D. Sylvan, "Expert consensus on the economics of climate change," Institute for Policy Integrity – New York University School of Law, Tech. Rep., 2015.

- [83] Y. Wang, J. Zhang, M. Ma, and X. Zhou, "Survey on driverless train operation for urban rail transit systems," *Urban Rail Transit*, vol. 2, no. 3–4, p. 106–113, 2016.
- [84] N. Lanzetti, M. Schiffer, M. Ostrovsky, and M. Pavone, "On the interplay between self-driving cars and public transportation," *arXiv preprint arXiv:2109.01627*, 2021.
- [85] G. Zardini, N. Lanzetti, L. Guerrini, E. Frazzoli, and F. Dörfler, "Game theory to study interactions between mobility stakeholders," in *2021 IEEE International Intelligent Transportation Systems Conference (ITSC)*, 2021, pp. 2054–2061, best Paper Award (1st place).
- [86] A. Zanardi, G. Zardini, S. Srinivasan, S. Bolognani, A. Censi, F. Dörfler, and E. Frazzoli, "Posetal games: Efficiency, existence, and refinement of equilibria in games with prioritized metrics," *IEEE Robotics and Automation Letters*, vol. 7, no. 2, pp. 1292–1299, 2022.
- [87] T. Maheshwari, "An urban design response to the technological shift in transportation: How to conduct urban design with vehicle automation, sharing and connectivity," Ph.D. dissertation, ETH Zurich, 2020.



Gioele Zardini (gzardini@ethz.ch) is a Ph.D. candidate at the Institute for Dynamic Systems and Control at ETH Zurich, under the supervision of Prof. Emilio Frazzoli. He received the B.Sc. and the M.Sc. degrees in mechanical engineering, with focus in Robotics, Systems, and Control from ETH Zurich in 2017 and 2019, respectively. He worked at nuTonomy (then Aptiv AM, now Motional) and was a visiting researcher at Stanford University and Massachusetts Institute of Technology. His current research interests include the co-design of complex

systems (all the way from future mobility to embodied intelligence), compositionality in engineering, planning and control, and game theory. He is the recipient of the Best Paper Award (1st Place) at the 2021 IEEE International Conference on Intelligent Transportation Systems.



Nicolas Lanzetti (lnicolas@ethz.ch) is a Ph.D. candidate at the Automatic Control Laboratory at ETH Zurich, under the supervision of Prof. Florian Dörfler. He received the B.Sc. and the M.Sc. degrees in mechanical engineering, with focus in Robotics, Systems, and Control from ETH Zurich in 2016 and 2019, respectively. He was a visiting researcher at Massachusetts Institute of Technology and Stanford University. His current research interests include optimal transport and gradient flows in the Wasserstein space, with applications in robust optimization and

game theory. He is the recipient of the Willi Studer Prize, the ETH Medal and the SVOR/ASRO award for his Master's thesis, and the Best Paper Award (1st Place) at the 2021 IEEE International Conference on Intelligent Transportation Systems.



Andrea Censi (acensi@ethz.ch) is the deputy director of the Dynamic Systems and Control chair at ETH Zurich, director of the Duckietown Foundation, and founder of Zupermind. He obtained a M.Eng. degree in Control and Robotics from the University of Rome, "Sapienza", and a Ph.D. from California Institute of Technology. He has been a research scientist at the Massachusetts Institute of Technology, and the Director of Research at Aptiv Autonomous Mobility (now Motional). He has been the recipient of NSF and AFRL awards.



Emilio Frazzoli (efrazzoli@ethz.ch) is a Professor of Dynamic Systems and Control at ETH Zurich. Until March 2021, he was Chief Scientist of Motional, the latest embodiment of nuTonomy, the startup he founded with Karl Iagnemma in 2013. He received the Laurea degree in aerospace engineering from the University of Rome, "Sapienza", in 1994, and the Ph.D. degree in Aeronautics and Astronautics from the Massachusetts Institute of Technology in 2001. Before joining ETH Zurich in 2016, he held faculty positions at the University of Illinois, Urbana Champaign, the University of California, Los Angeles, and at the Massachusetts Institute of Technology. His current research interests focus primarily on autonomous vehicles, mobile robotics, and transportation systems. He led the research groups that first demonstrated an autonomous mobility service to the public, and performed the first analysis of the social and economic impact of such a service, based on real transportation data.

He was the recipient of a NSF CAREER award in 2002, the IEEE George S. Axelby award in 2015, the IEEE Kiyo Tomiyasu award in 2017, and has been named an IEEE Fellow in 2019.



Marco Pavone (pavone@stanford.edu) is an Associate Professor of Aeronautics and Astronautics at Stanford University, where he is the Director of the Autonomous Systems Laboratory and Co-Director of the Center for Automotive Research at Stanford. He is currently on a partial leave of absence at NVIDIA serving as Director of Autonomous Vehicle Research. He received a Ph.D. degree in Aeronautics and Astronautics from the Massachusetts Institute of Technology in 2010. His main research interests are in the development of methodologies for the

analysis, design, and control of autonomous systems, with an emphasis on self-driving cars, autonomous aerospace vehicles, and future mobility systems. He is a recipient of a number of awards, including a Presidential Early Career Award for Scientists and Engineers from President Barack Obama, an Office of Naval Research Young Investigator Award, a National Science Foundation Early Career (CAREER) Award, a NASA Early Career Faculty Award, and an Early-Career Spotlight Award from the Robotics Science and Systems Foundation. He was identified by the American Society for Engineering Education (ASEE) as one of America's 20 most highly promising investigators under the age of 40. He is currently serving as an Associate Editor for the IEEE Control Systems Magazine.